Consortium

for

Small-Scale Modelling

Newsletter

May 2023   No.22

Table of Contents

The editorial of this 22nd issue of the COSMO Newsletter is the first one since 2019 with a group picture. It is the one of the 24th COSMO General meeting in Athens 2022. A group picture by itself might not have been considered as more than a usual habit in previous years. This time, however, it is a symbol for the return to in-person meetings which we missed from the pre-Covid years. The COSMO general meeting has been a great success for both the scientific exchange and the team building within the COSMO community. While we have learnt to move a lot of our discussions, meetings and planning to the virtual space in recent years, the COSMO GM 2022 clearly demonstrated that regular in-person meetings are essential for the successful cooperation within such a consortium.

Of course, the cooperation within COSMO will make use of purely online or hybrid meetings from now on (admittedly also due to significant cuts in travel budgets for some COSMO members). But such meetings can provide advantages. For example a temporal decoupling of the different working group meetings thereby allowing for a broader participation. This was hardly realizable with the previous concept of only in-person meetings. Moreover, the ICCARUS 2023 was held in a hybrid format giving more participants the opportunity to follow the presentations. One intention of this hybrid approach was to ease and foster the cooperation between COSMO and ICON communities, in particular in thematic working group meetings which opened up the standard COSMO WG discussions for the larger community. In this sense, ICCARUS 2023 can be considered as part of the efforts towards a successful transition of COSMO consortium to the ICON model, which is ongoing. After successful installation of deterministic forecasts with ICON for the COSMO members in recent years, more and more meteorological services of COSMO already started with ICON-LAM-based ensemble forecasts or are currently preparing this step.

Another important change related to the transition to the ICON model is the adaption of the COSMO licence. An ICON usage licence is now available to be used by any NHMS for its official duty. The COSMO consortium supports the use of ICON by its new ICON-COSMO Support Licence. The support licence is subject to a licence fee which depends on the gross domestic product per capita (GDPpc) of the licensee's country. The annual fee currently (April 2023) ranges between €4,800 and €20,000 with the possibility of a full waiver of the fee for GDPpc below a defined threshold. It is an honour to welcome the meteorological service of the Republic of Yemen as the first new licensee under the modified licence structure. To prepare the future support for COSMO-ICON licensees, the Priority Project C2I4LC ('Establishing COSMO to ICON migration for Licensees' Countries') started in September 2022 and is led by Bogdan Maco of the Romanian Meteorological Service NMA. A core task of the preparatory PP is the set up of a ticketing system with a single point of contact for support requests.

There are two more new projects which started in recent months. The Priority Project CARMEns ('Cosmo Application of Rfdbk/MEC on ENS') started in September 2022 under the lead of Amalia Iriza-Burca (NMA) and extends the successful implementation of the MEC-Rfdbk system for verification of deterministic forecasts (previous PP CARMA) to forecasts of ensemble prediction systems. In March 2023, the Priority Task EPOCS ('Evaluate Personal weather station and Opportunistic sensor data CrowdSourcing') started and is led by Joanna Linkowska of the Polish Meteorological Service IMGW. Its aim is the assessment of the applicability of alternative weather data acquired by the Personal Weather Stations and other Opportunistic Sensors into research and operations activities at the level of national weather services. The main focus is on the development and testing of data quality control algorithms.

In this issue of the newsletter, the routinely performed evaluation of COSMO and ICON models over the Common Areas is presented for 2021-2022. There are two research contributions in COSMO Newsletter No 22. The one is a model sensitivity study of ICON for the Central Mediterranean area as further important input for the transition from COSMO to ICON model. The other contribution reports on operational forecasts for air dispersion of hazardous pollutants as a topic of actual relevance.

I would like to thank all contributors to the COSMO Newsletter No. 22 and the editorial team, in particular Mihaela Bogdan and Massimo Milelli, for the effort put into setting up this issue of the Newsletter.

Looking forward to the COSMO General meeting in Poland in September 2023,

Gebhardt Christoph
COSMO Scientific Project Manager

Figure 1: Participants of the 21th COSMO General Meeting in Athens, Greece

Operational forecasts for air dispersion of hazardous pollutants based on results of the COSMO model.

ANDRZEJ MAZUR

Institute of Meteorology and Water Management – National Research Institute
61 Podlesna str., PL-01673 Warsaw, Poland

1 Introduction

The project developed at the IMWM-NRI is intended to help in determining the response to the occurrence of a potential danger to Poland, related to at least two types of threats:

1. anthropogenic threats, resulting mainly from incidents in nuclear power plants (NPPs – cf. Fig. 1) in neighboring countries, as well as other disasters or accidents of the nature of emission incidents, causing contamination of the environment with toxic (more generally: dangerous) substances ;

2. natural threats, such as volcanic eruptions and eruptions, and their impact on broadly understood safety, including e.g. the safety of air transport.
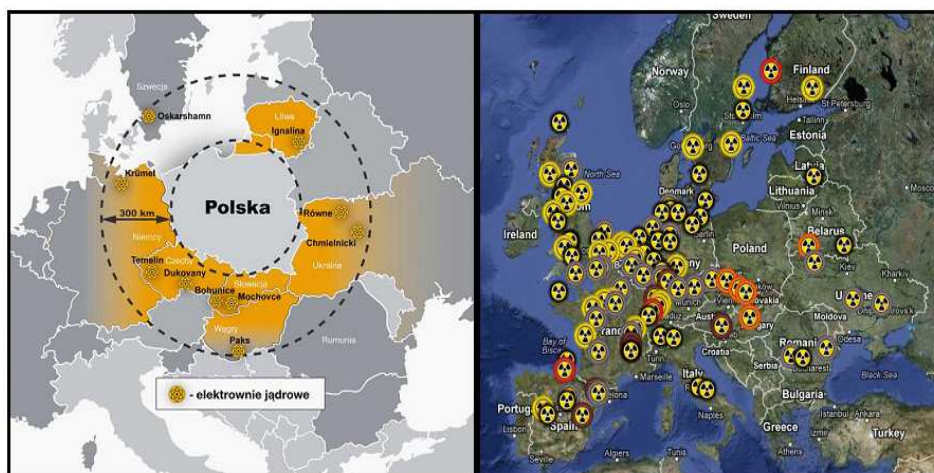
Figure 1: Left – NPP within 300 km from Poland (Mazur, 2015). Right – High-risk reactors in Europe. Red – the type used in Fukushima; Orange – inadequate security; Yellow – older than 30 years; Brown – seismically active region. Other: Gray – under construction; Black – turned off (status – end of 2015 yr.)

In terms of safety, the key issue is information – including forecasts – if/how the territory of Poland may be endangered as a result of a hypothetical accident in selected NPP(s) or of a release of another contamination.

At IMWM-NRI a system for forecasting – in operational mode – the dispersion of pollutants from locations in the COSMO model domain has been prepared. Two models (Lagrangian – trajectory and Eulerian – field) are complementary in terms of information on dispersion of pollutants. 1. The Lagrangian model: three-dimensional trajectory calculated as a solution for the following set of equations (Potter, 1979):

$$\frac{dx}{dt} = u(x;t)$$

where x=x(t) – 3D coordinates of the trajectory point; u – 3D windspeed field.
Solution, understood as a change of point's location is given by the following procedure:

$$\Delta x_0 = u(x_0;t_0) \cdot \Delta t$$

With iterative correction and iteration index i=1,3:

$$\Delta x_i = \frac{\Delta x_0 + u(x_0 + \Delta x_{i-1};t+\Delta t)\cdot \Delta t}{2}$$

Finally (for i=N=3):

$$x(t + \Delta t) = x(t) + \Delta x_N$$

2.Eulerian model

General equation of dispersion (including horizontal advection and vertical diffusion) of contamination concentration c may be written as:

$$\frac{\partial c}{\partial t} + \frac{\partial uc}{\partial x} + \frac{\partial vc}{\partial y} = \frac{\partial}{\partial z}\left(K_v \frac{\partial c}{\partial z}\right) + G$$

where u, v – 2-D windspeed field; K_v – tensor of turbulent diffusion (vertical component), G – contamination's emission and removal (wet- and dry deposition). Solution is calculated separately for horizontal advection – with Flux Correction method (class of AFP – Area Flux Preserving approaches), vertical diffusion – with semi-explicit Crank-Nicholson's method (cf. Bott, 1989, Potter, ibid.). Both types of models are used in the system, giving complementary information.

2 Concept, goals and results

Main general goal of the work was to increase an overall level of Poland's safety in the context of nuclear installations located in neighboring countries, safety and fluency of air traffic over Poland in the event of volcanic eruptions (introduction of a periodic ban on flights over Poland), the possibility of reacting to the occurrence of other releases of hazardous, toxic substances, etc.

The effect of implementation became a system for forecasting and informing about the possible effects of incidents related to nuclear accidents of a wide scale of intensity or volcanic eruptions located throughout Europe, which may result e.g. in the introduction of a flight ban over selected areas of the continent, including Poland, or any other release of dangerous or toxic substances into the atmosphere.
The results may be used to determine actions and responses for events of this kind. In Figure 2 an example of the results is presented.
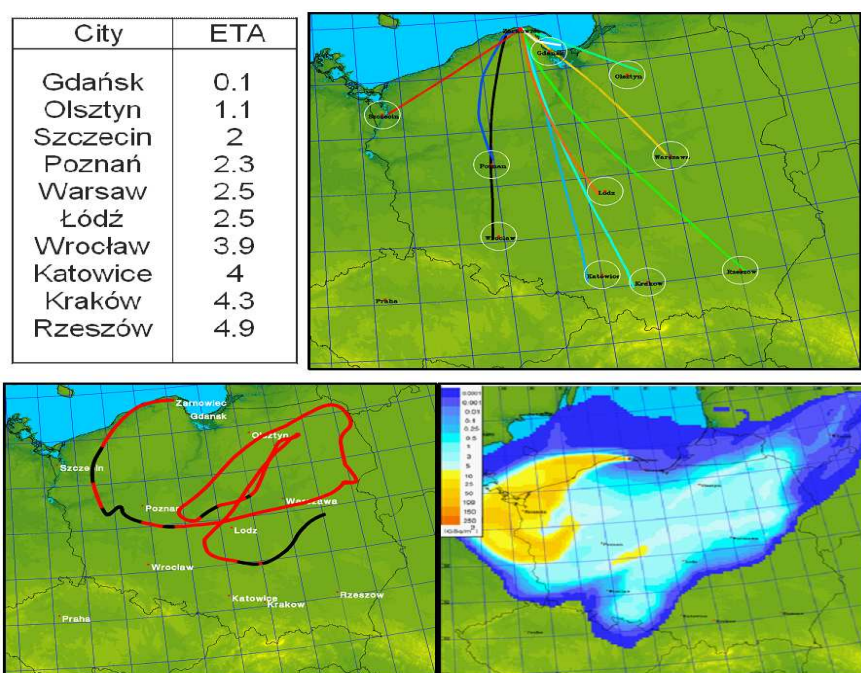
Figure 2: Assessment of the impact of the future Polish NPP; climatological data 2001-2010 (Mazur, ibid.). Upper left – estimated fastest times of arrival (ETA, hours) of contamination cloud to main Polish cities. Upper right – paths of fastest trajectories, as computed with Lagrangian model. Lower left – the trajectory with the longest course over the territory of Poland. Lower right – results of Eulerian model for the case of the release for longest trajectory.

Another example was an assessment of the impact from Chernobyl NPP with climatological data 2001-2010, as shown in Figure 3. The results showed that the "real case" of 25-26 of April 1986 was a special not only because of the catastrophic intensity of the release, but also because of spatial scale and range of the atmospheric dispersion. From climatological data (2001-2010), the probability of impact (Figure 3, left) was relatively much smaller for western Europe then for western part (or eastern Europe) of USSR. Yet, the mean estimated time of arrival (ETA again) was in general in line with reality. For example, contamination cloud came to Poland within 24 hours, as modeled.
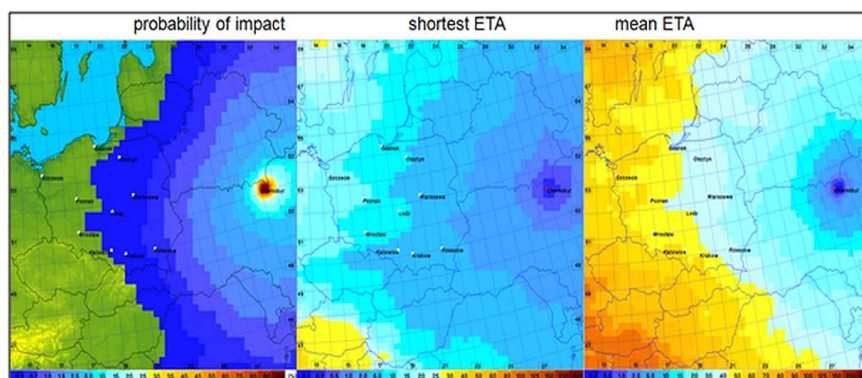
Figure 3: Assessment of the impact from Chernobyl NPP; climatological data 2001-2010, see explanations in text (Mazur, ibid.).

In basic setup, operation forecasts of air dispersion of pollutants was computed over a domain centered over Poland with spatial resolution of 7km, 385x321 grid points, as shown e.g. in Figure 4.
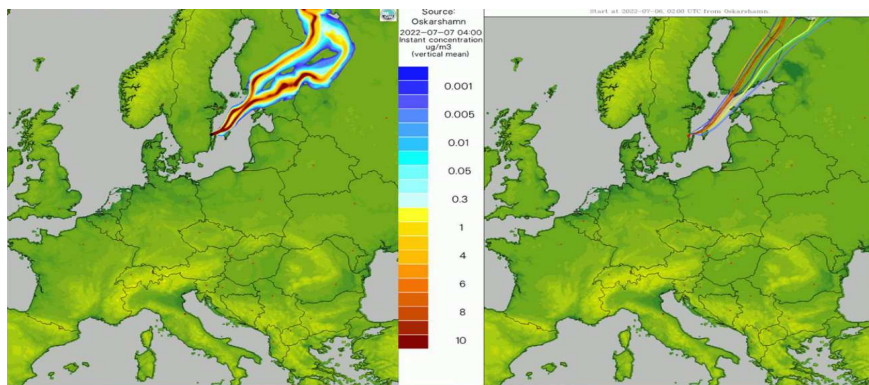
Figure 4: Domain for basic operational setup – an example of operation forecast of air dispersion of nuclear cloud from NPP in Oskarshamn, Sweden. Left – vertical mean of instant concentration (ug/m3), calculated with Eulerian model. Right – respective trajectories computed with Lagrangian model.

Due to the ongoing war in Ukraine, and especially situation with Ukrainian NPPs, the domain had to be extended by about 20 at least in the eastern direction, as shown in Figure 5. The extended domain covers the entire territory of Ukraine and its closest vicinity.
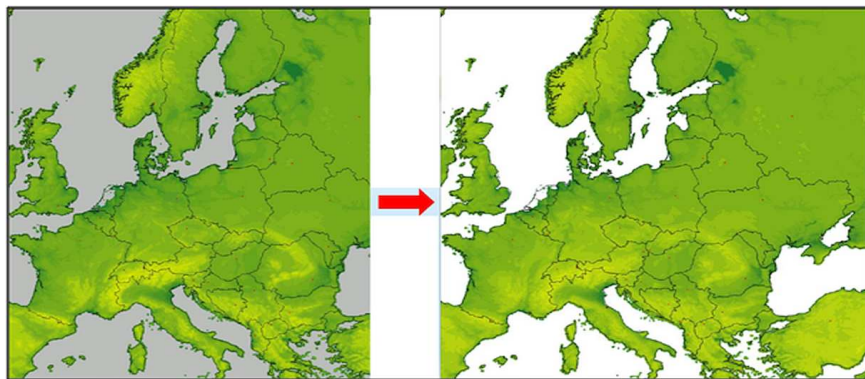
Figure 5: Extension of domain due to war in Ukraine and situation in nuclear power plants.

In Figure 6 the example results of calculation for special case – emission (or release) from NPP In Enerhodar, east of Ukraine.
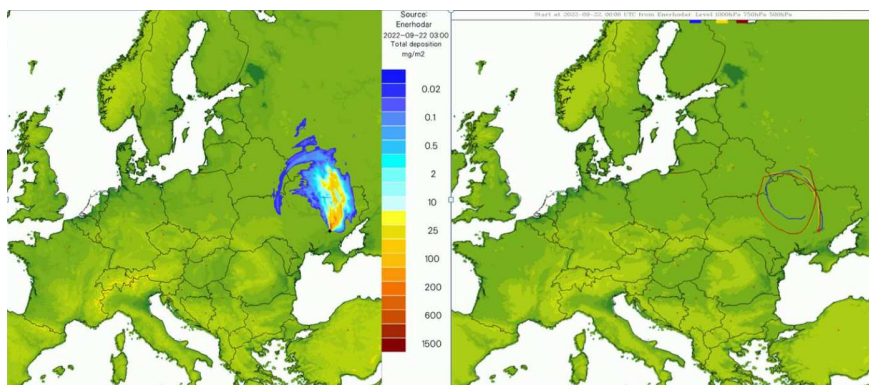
Figure 6: Domain for modified operational setup – an example of operation forecast of air dispersion of nuclear cloud from NPP in Enerhodar, Ukraine. Left – total deposition (mg/m2), calculated with Eulerian model. Right – respective trajectories computed with Lagrangian model

3 Summary

The entire history of mankind is full of emission incidents or even disasters, both resulting from military and peaceful uses, both anthropogenic and natural. Below are provided some examples (cf. Mazur, ibid.).

- October 1957, accident in Windscale reactor (UK): contaminated 500 km2 of the area around the NPP; similarly to the Chernobyl accident – a result of an unfortunate combination of many factors;

- April 1986, explosion and fire of Chernobyl reactor; commonly believed – a catastrophe on a global scale both in terms of the amount of the release and of it spatial extent;

- April 2010, eruption of Eyjafjallajökull volcano in Iceland, flight bans, threat to air traffic over Europe;

- March 2011, the disaster at the Fukushima NPP – the result of an earthquake, the impact of the tsunami wave and a confluence of unfortunate circumstances and human errors;

- September to December 2021, Cumbre Vieja volcano eruption – a hundred days of emission of volcanic ashes/sulfur compounds.

This list is definitely not complete. That is why there is a need for efficient systems that would respond to a crisis situation – a threat to the natural environment or human activity. It is important to prepare tools that allow to react and/or minimize the negative effects of possible accidents/releases. Such systems (Bartzis et al., 2000; Hoe et al., 2009) are to provide support – an information on the further development of events, the forecasted state of the environment and the negative impact of various factors on human society within the range of such impact.

The motto for this work was a Latin maxim: *"Si vis pacem, para bellum!"*. It means that we should be prepared for various difficult situations, even if they never happened.

References

1. Bartnicki J., Salbu B., Saltbones J., Foss A., 2005, Analysis of Atmospheric Transport and Deposition of Radioactive Material Released During a Potential Accident at Kola Nuclear Power Plant. Research Report No. 10, ISSN 1503-8025. Norwegian Meteorological Institute, Oslo, Norway.

2. Bartzis J.,Ehrhardt J., French S., Lochard J., Morrey M., Papamichail K.N., Sinkko K., Sohier A., 2000, Rodos: Decision Support for Nuclear Emergencies. In: Zanakis S.H., Doukidis G.,

3. Zopounidis C. (eds) Decision Making: Recent Developments and Worldwide Applications. Applied Optimization, vol 45. Springer, Boston, MA

4. Bott A., 1989, A positive definite advection scheme obtained by nonlinear renormalization of the advective fluxes. Mon.Wea.Rev., 117, 1006-1015.

5. Hoe S., McGinnity P., Charnock T., Gering F., Jacobsen L.H.S., Sørensen J.H., et al., 2009, ARGOS decision support system for emergency management. In: Proceedings of the 12th International Congress of the International Radiation Protection Association. IRPA, Buenos Aires, Argentina.

6. Mazur A., 2015, Project RIOT – Ring of Threats – as an example of Decision Support System (DSS). Concept and Realization. Meteorol. Hydrol. Water Manage. 2015, vol. 3, no. 2, 39-47. DOI: https://doi.org/10.26491/mhwm/60273

7. Potter D., 1973, Computational Physics. J.Wiley & Sons.

COSMO/ICON-LAM evaluation over Common Areas: 2021-2022

COSMO WG5: Verification and case studies

Flora Gofa (fgofa@hnms.gr)

1 Overview

Verification results of statistical indices for main weather parameters are derived using the operational COSMO and ICON-LAM model implementations in each service. The domain (common), the resolution, the statistical scores/methods and the graphical representation approaches, are decided on an annual basis from WG5. A common verification software is used for both point wise and neighborhood approach verification which allows for a homogeneous, standardized and objective way to apply, calculate and present the verification scores. The outcome of this activity provides a basis to monitor the performance of the operational models implementation and track the systematic errors. Since the introduction of ICON-LAM in the operational forecast procedure of some services, special focus is given to the relative performance of the two models. In this report, statistical results of JJA-2021 up to MAM 2022 model performance are presented.

COSMO consortium has developed a standardized procedure for assessing the performance of its partners models, which involves evaluating verification scores across common areas, using the same observations and methods, and since this year, the same verification software. The verification results for key weather parameters, generated using the operational COSMO and ICON-LAM model implementations, are compared in each service, while the decision about the specific domain, resolution, statistical scores and methods, as well as the graphical representation of the scores is made on an annual bases by WG5. The results of this analysis, along with long-term trends, are presented every September during the GM plenary session, providing a means to track model performance. The use of common verification software ensures a standardized and objective approach to applying, calculating, and presenting verification scores, with observation data preparation and seasonal statistics calculated according to guidelines (`https://www.cosmo-model.org/content/tasks/verification.priv/common/reports/CP-2021-2022.pdf`)Guidelines 2021/22 developed annually by WG5. ICON-LAM models statistical results are included from any of the various services that use the model operationally.

The verification approach is primarily based on point-wise comparison that is performed with the use of Feedback Files generated by MEC software and analyzed from Rfdbk R-based libraries. For 2021-2022, conditional verification is also applied on temperature forecasts, meaning the interdependency of temperature and cloudiness with respect to model performance. Finally, neighborhood (spatial) methods are applied to precipitation fields and this year also to total cloudiness as it is shown on following paragraph. Selective verification results of COSMO and ICON-LAM models over Common Area 1 (ComA1) and Area 2 (ComA2) are presented below while the complete selection of statistical results can be found in `https://www.cosmo-model.org/content/tasks/verification.priv/common/reports/CP-2021-2022.pdf`Guidelines 2021/22.

2 Areas of Verification

The areas and specifications for model performance evaluation are presented below. In ComA-1, models with coarser resolution are included, while the higher resolution COSMO and ICON-LAM models are compared over ComA-2 (Table below).
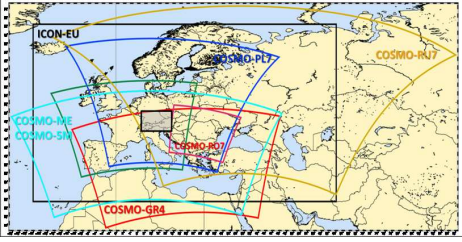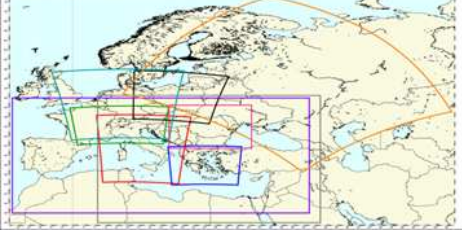
ComA-1 Area/Specs	
	00UTC Forecast runs Forecast Horizon: 72h Seasonal: JJA20, SON20, DJF21, MAM21
Models	**Global LAMS** ICON global DWD: ICON-EU COMET: COSMO-ME HNMS: COSMO-GR4 ARPA-E: COSMO-5M IMGW-PIB: COSMO-PL7
ComA-2 Area/Specs	
	W10.963, S46.597, E17.437, N49.550 00UTC Forecast run Forecast Horizon: 48h Seasonal: JJA20, SON20, DJF21, MAM21
Models	**LAMS** DWD: ICON-D2 COMET: COSMO-IT, ICON-IT HNMS: ICON-GR2.5 ARPA-E: COSMO-2I IMGW-PIB: COSMO-PL2.8, ICON-PL2.5 MCH: COSMO-1E, COSMO-2E IMS: ICON-IMS

Table 1: Specifications of ComA-1, ComA-2 verification areas

3 Selective Verification Results

3.1 Point-wise verification for Com-A1

The models are evaluated in terms of Mean Error and Root Mean Square Error indices for the continuous parameters, using SYNOP observations over the Common Areas 1 and 2 domains. Summary plots of main weather parameters for coarser models are shown in Figure 1, selectively for DJF2022 season. For ICON models (ICON, ICON-EU, ICON-RU), the bias diurnal cycle is weaker and RMSE values are reduced for T2m. RMSE is wind speed is slightly higher in warm hours of the day and comparable for all models in all seasons. The nighttime WS overestimation however which is a typical systematic error with COSMO models, is not apparent on ICON-LAM models, which exhibit a much weaker ME daily cycle, and an almost underestimation. RMSE for PS is reduced for ICON models.

However, the tendency of PS RMSE increase with forecast time for all seasons appears also with ICON models while the bias in DJF, exhibits negative values for ICON models, in contrast to positive for COSMO. TCC RMSE values and bias diurnal cycles are similar in behavior with reduced RMSE values for ICON models with RMSE maximum values at night. With respect to ME however, ICON models produce higher underestimation in DJF during midday and slightly higher overestimation at night, for all seasons.

Figure 1: RMSE (first row) and ME (second row) indices for (from left to right) Total Could Cover, Wind Speed, 2m Temperaure and Pressure calculated over ComA-1 (DJF2022).

3.2 Point-wise verification for ComA-2

For a better comparison among COSMO and ICON-LAM higher resolution models over ComA-2, they are grouped together in order to detect general tendencies or differences that can be attributed to the various implementations. Below statistics for selected parameters are presented for DJF 2022.
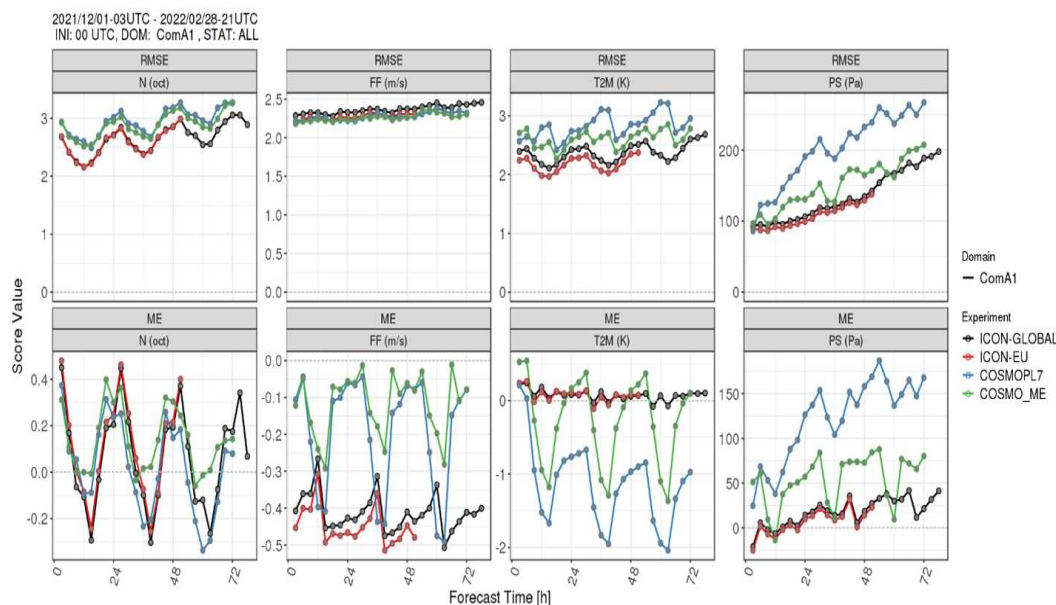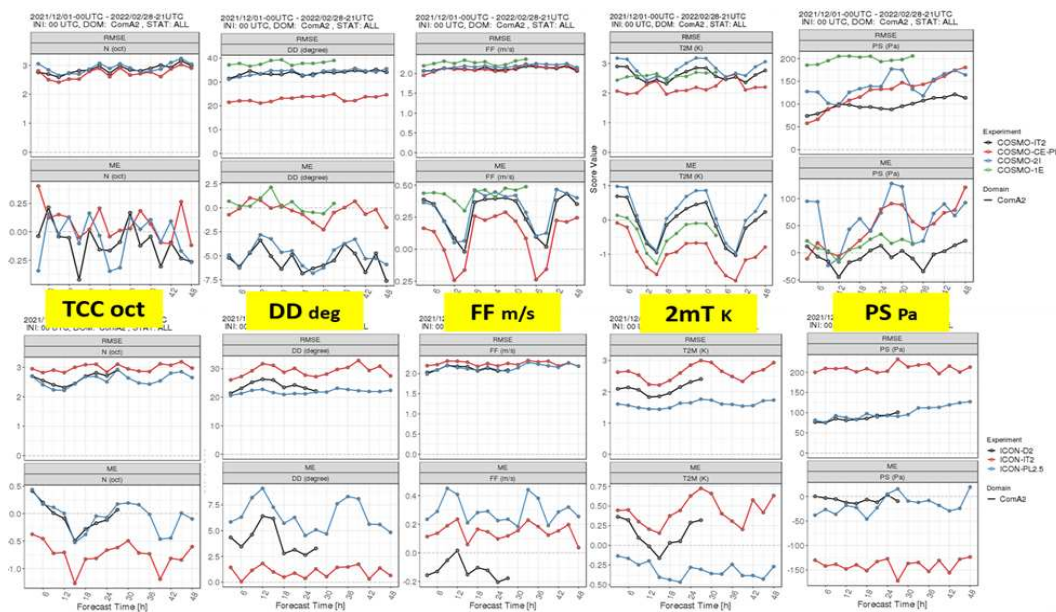
Figure 2: RMSE (first row) and ME (second row) indices for (from left to right) Total Could Cover, Wind dir, Wind Speed, T2M and Pressure calculated over ComA-2 (DJF2022)

For 2mT, one distinct difference, which is also consistent with coarser resolution models, is the ME reduced diurnal variability for ICON-LAM models, which is shown in DJF, with values closer to zero. The RMSE diurnal variation amplitude is comparable for the two sets of models with RMSE values for ICON models exhibiting an overall reduction.

For wind speed, The ME diurnal variation is weaker for ICON models and the tendency for overestimation is not as distinct with ICON-LAM implementations. Moreover, the bias diurnal variability is shifted among the two sets of models, with ICON overestimation in the early morning hours, while COSMO models bias is positive around evening hours.

The RMSE error cycle and range are similar for all models and no clear impact can be shown with either COSMO or ICON-LAM models. For wind direction, the reduction in error can be partially associated with Pressure error reduction. For Total Could Cover, the performance trend is not clear among ICON-LAMs as there is a significant spread while RMSE values are similar for both sets of models.

3.3 Wind performance

In this section, special focus is given to wind related properties in terms of their performance over ComA-1 and ComA-2 domains. Specifically, RMSE and ME indices are calculated for wind speed, wind direction and hourly wind gust.

Figure 3: RMSE (first row) and ME (second row) indices for Wind speed, Wind Gust and Wind direction over ComA-1 (MAM2022).
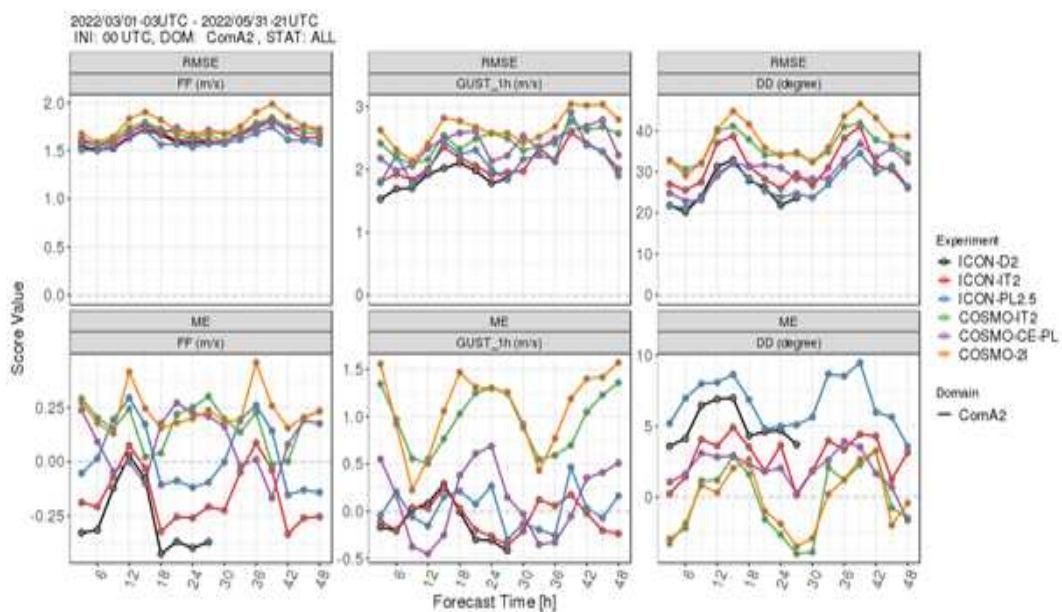
Figure 4: RMSE (first row) and ME (second row) indices for Wind speed, Wind Gust and Wind direction over ComA-2 (MAM2022).

As expected, the resolution-dependence is very clear for wind speed and direction. With respect to model effect on wind properties, all three parameters performance is grouped accordingly. For wind gust, a more significant reduction of the overprediction tendency with higher resolution ICON-LAM models while with wind speed the common trend of overprediction for coarser models is only changed in phase with ICON models (max over evening hours). In higher resolution models, wind speed is overpredicted with COSMO models and underpredicted with ICON-LAMs. Large diurnal cycle for ME for all wind properties is exhibited that can be related to boundary layer mixing in higher resolutions, with differences in phase for the maxima among COSMO/ICON implementations.
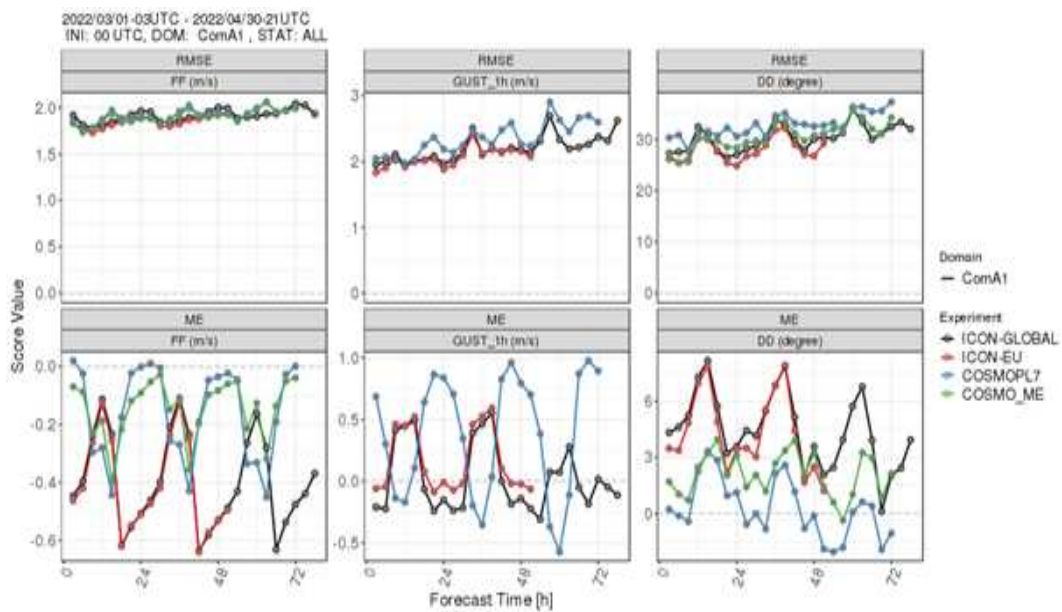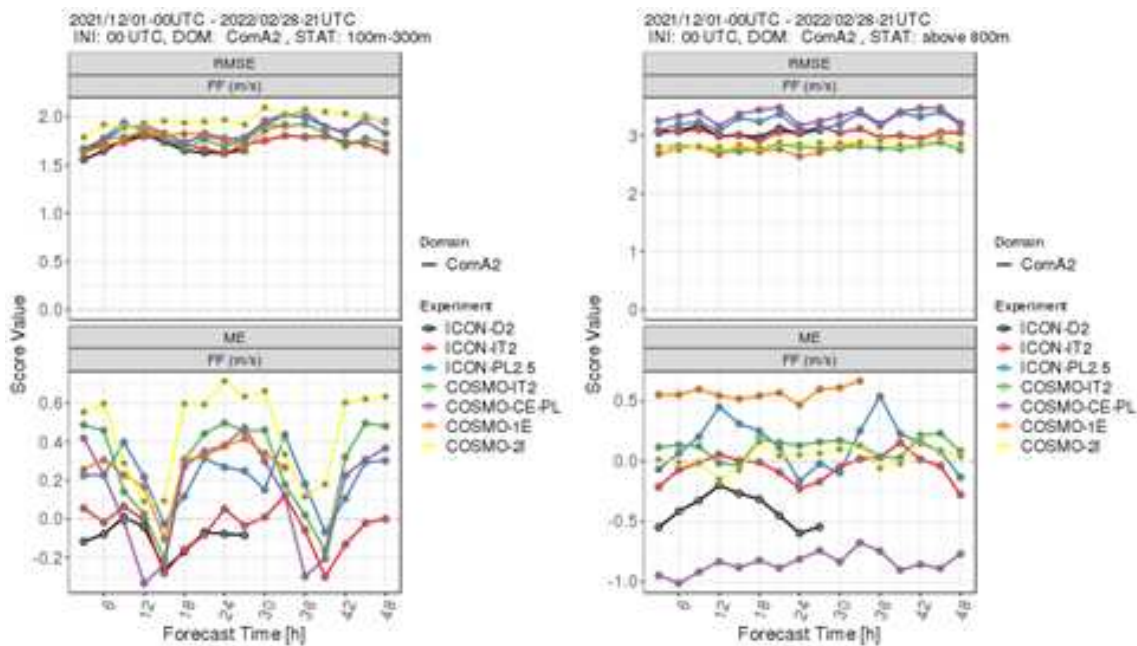
Figure 5: RMSE (first row) and ME (second row) indices for Wind speed, Wind Gust and Wind direction over ComA-2 (MAM2022).

Focusing in two different stratifications, one below 300m and one above 800m, there is a clear altitude dependence in performance for all seasons. The RMSE grows significantly in higher elevation points with sightly higher values for ICON-LAMs, with a general underestimation of wind speed while for lower elevations COSMO models tend as shwn also before to overestimate values some trend that is reduced with ICON-LAMs.

3.4 Temperature/Cloudiness performance dependence

The dependency of 2m temperature performance to total cloudiness is analysed in this section. Specifically, statistical indices are calculated for temperature when cloudiness is less than 25% (near clear sky conditions) and for cloudiness higher that 75% (near overcast conditions). Both conditions are imposed on observations. The outcome of this test selectively for one season (DJF2022) is presented in Figure 6. The RMSE values of 2mT are found in clear sky conditions, and lower errors when overcast conditions are examined compared to the total sample results. The diurnal variability of error is stronger for COSMO models when few/no clouds are present. When the relative performance of models is analysed, it is clear that there is a significant improvement of 2mT forecasts with ICON models in all seasons and cases. For the summer (not shown here), there is a distinct overestimation of 2mT mainly during cloudy days, which seems to be higher in some ICON-LAMs. Worst warming happens during midday while at night the effect is reverse in clear days with cooler models.
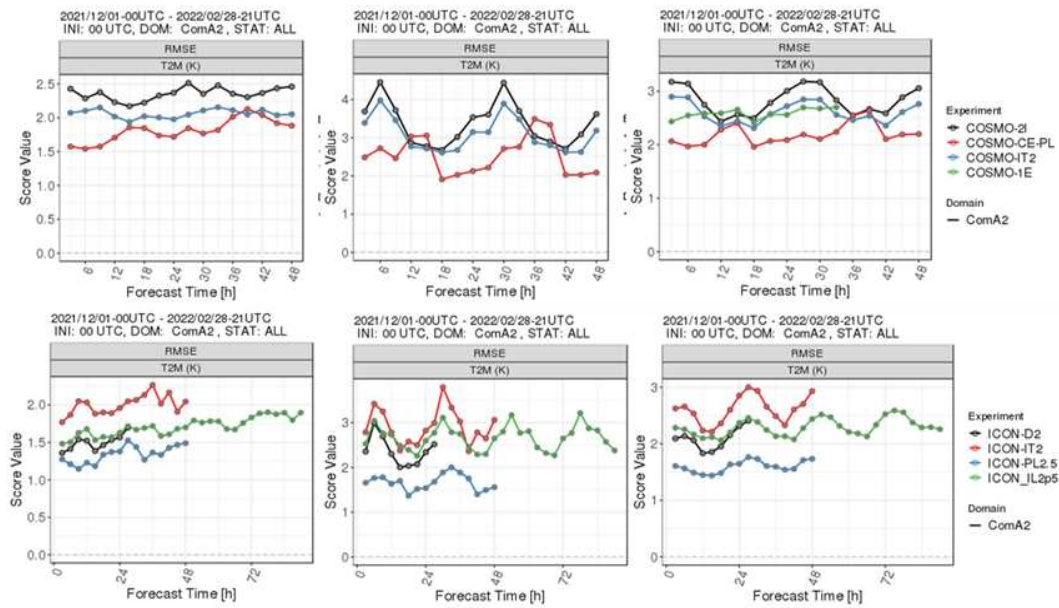
Figure 6: RMSE (top) and ME (bottom) for 2mT for overcast conditions (left), clearsky conditions (middle) and for all cases (DJF2022).

3.5 Cloudiness performance

Verifying cloud forecasts from NWP models has proved to be a difficult task because of the complex three dimensional structures of clouds, and lack of routine observations adequate for the purpose. Furthermore, it is not just of interest in its own but also has a major impact on other parameters, such as temperature and solar radiation. As it is highly variable in terms of time and location, it is difficult to forecasted but also verified. The main reason is the spatial representativeness mismatch between forecasts and SYNOP observations that are widely and almost exclusively used for this purpose. The area covered by visual observation typically varies between 10 and 100 km around a station, depending on visibility and topography. In this section, cloudiness is evaluated both point-wise and spatially with the use of satellite estimates.

3.5.1 Verification against SYNOP

As with other continuous parameters, COSMO and ICON-LAMS are evaluated against SYMOP observations over the common areas systematically. The seasonal statistical Mean Errors for winter and summer 2022 are presented in Figure 7, grouped separately for the two models. The TCC bias difference among the two sets of models is clear, with ICON models exhibiting a diurnal cycle with constant underestimation of observed values especially during the warm hours for both seasons. In the contrary, COSMO models exhibit mainly TCC overestimation while ICON models behavior is ambiguous. On the other hand, the RMSE diurnal cycle is similar for both sets, while higher values of errors are present during night hours.
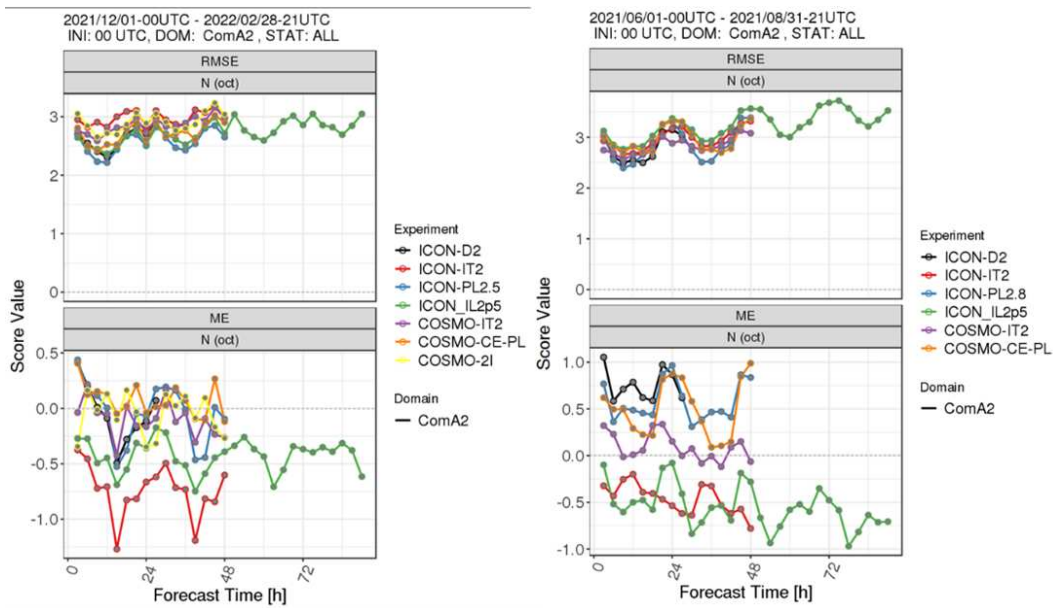
Figure 7: RMSE (top) and ME (bottom) for Total Cloud Cover for DJF 2022 (left column) and JJA2021(right column) over ComA-2.

3.5.2 Verification against NWC-SAF

Due to restrictions that were mentioned before regarding the representativeness of cloudiness SYNOP observations, a first approach evaluating this parameter against satellite estimates was initiated as part of WG5 common plot activity. In detail, NWC-SAF cloud mask fields (0.025 degrees) were retrieved and converted to TCC octants to be used in the gridded application of FSS score.
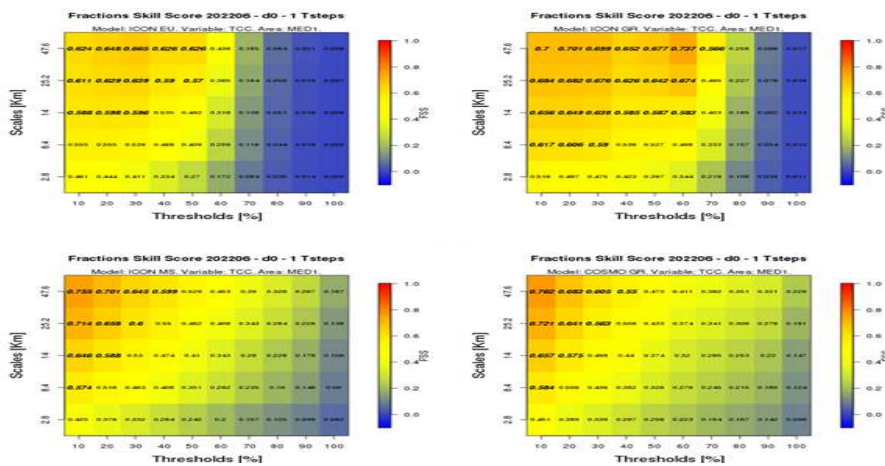
Figure 8: FSS for TCC for June 2021 over the east Mediterranean area.

As the quite restricted area of ComA-2 was too small for the analysis of cloud field, an extended verification area over east Mediterranean was used for a stratification of the operational models that covered this domain, while the time period was June 2022. The spatial verification approach can reveal the scales that cloudiness forecasts can be useful, by relaxing the criterion of strict point to point comparison.

Overall, for this experiment the useful scales proved to be for windows that forecast information is averaged

in higher than 14km windows while and cloud coverage less than 30% cloudiness the performance was most successful.

The most striking result that was consistent with the unclear performance of models against SYNOP data, was that COSMO models at high percentages of TCC, outperform ICON-LAMs.

3.6 6h Precipitation performance evaluation

The station-based 6h accumulated precipitation forecasts are evaluated in terms of categorical indices for different thresholds. JJA2021 and DJF2022 results for ETS, POD and FAR are presented in Figures 9a,b.
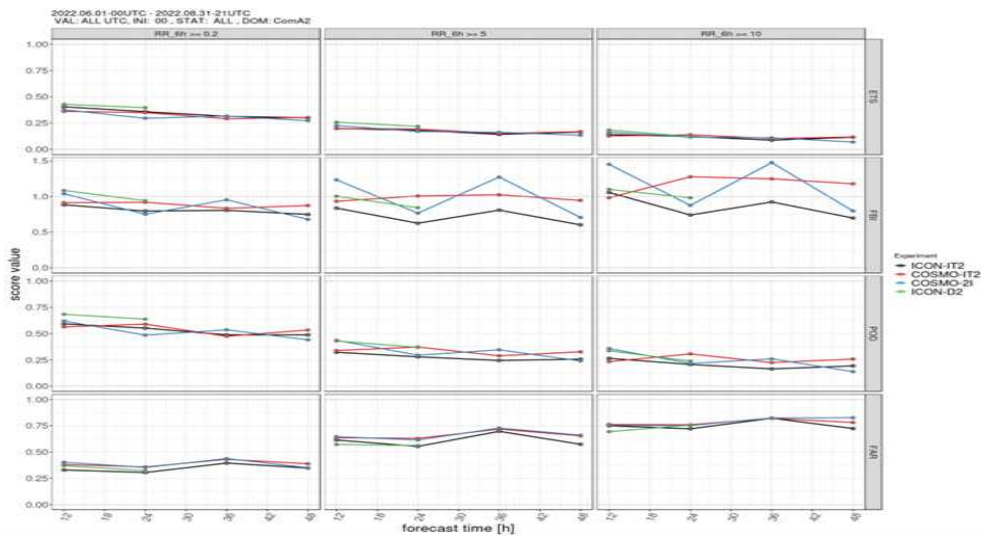
Figure 9: 6h accumulated precipitation indices for different thresholds. From top to bottom (ETS, FBI, POD, FAR). From left to right (0.2, 5, 10mm) for JJA2021.
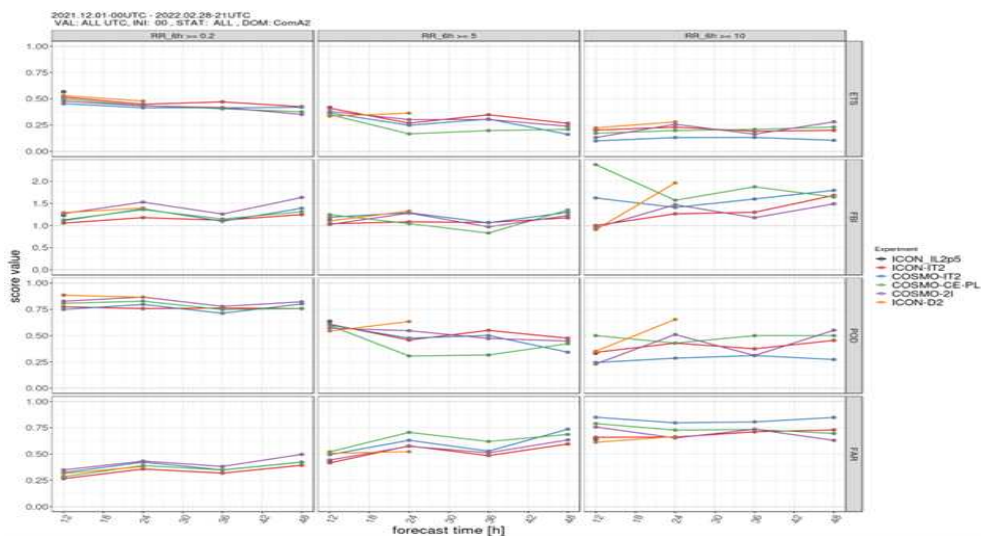
Figure 10: 6h accumulated precipitation indices for different thresholds. From top to bottom (ETS, FBI, POD, FAR). From left to right (0.2, 5, 10mm) for DJF2022.

As in previous years, scores trend worsen slightly with forecast time and significantly with increasing threshold. Differences among ICON and COSMO models are not so clear but separating the two different model groups there is a distinct small improvement in all scores with ICON-LAMS. More significant is the improvement during the summer period that was analysed.

3.7 Fuzzy 6h-Precipitation verification

This section presents fuzzy verification scores for ComA-2 compared to the OPERA network radar composites. The VAST COSMO software, which is based on Beth Ebert's fuzzy verification IDL code, was used for this task. The VAST main code utilizes txt gridded files for each weather parameter, and a preprocessing of input files is available with the help of LIBSIM software. The main indices used to summarize the spatial verification results are FAR, Fraction Skill Score (FSS), and POD, as shown in Figure 10.

These scores compare the forecast and observation (radar) 3-hour gridded precipitation fields on continuously increasing spatial windows and for varying precipitation thresholds. The results for three different thresholds (0.1, 5 and 10mm/3h) are presented for the first forecast day and for the three seasons (JJA21, SON21, DJF22).

The spatial verification approach shows a relatively improved skill of ICON-LAM models compared to COSMO ones in precipitation forecasts, especially with respect to FAR and FSS scores. However, for the POD score, as also extracted from the point-wise verification mainly for the smaller thresholds, the scores are slightly worse in some cases.
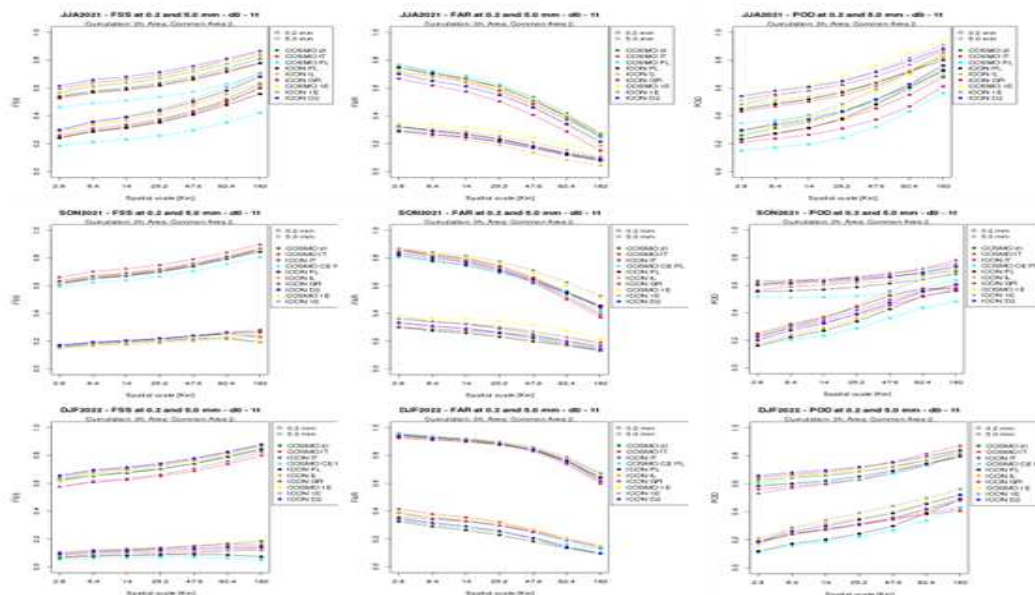
Figure 11: FAR (left), FSS (middle) and POD (right) 3h Precipitation scores for forecast day 1 for JJA21 (top row), SON21 (middle row) and DJF22 (lower row) calculated over ComA-2.

4 General Concerns

The WG5 common plot activity provides a good basis for fulfilling the minimum requirements of monitoring operational model performance of all participating services.

A detailed presentation of the verification findings were presented during General Meeting in September 2022 while the complete range of plots are available on `http://www.cosmo-model.org/content/tasks/verification.priv/default.htm`Verification tasks. As a general conclusion, improvement in performance in most cases/parameters analyzed with ICON-LAMs compared to COSMO implementations was derived from this year activity. There are however components that further model development is needed, as long-term biases are still present. The deviation among model performance is greater in ICON-LAMs than in COSMO models, revealing the need for further model tuning especially in high resolution scales.

On the Seasonal Sensitivity of ICON Model

E. Avgoustoglou[1], A. Shtivelman[2], P. Khain[2], C. Marsigli[3,4], Y. Levi[2] and I. Cerenzia[4]

[1] *Hellenic National Meteorological Service (HNMS),* [2] *Israel Meteorological Service (IMS),*
[3] *Deutscher Wetterdienst (DWD),* [4] *Arpa Emilia-Romagna (ARPAE)*

1 Introduction

Over the last few years, the local version of ICON model (Zängl etal, 2015, Prill etal, 2020) has gradually undertaken COSMO model on the operational mode of the Consortium Members. In addition to the complexities of installing the model to many different computer architectures as well as data assimilation issues, such an endeavour is quite challenging regarding the proper choice of the many model parameter values in order for the model to have the optimum performance. An important step towards this direction is to estimate the sensitivity of ICON model in reference to these parameters. Such an effort is addressed within the framework of the replacement of the currently operational COSMO-LEPS with its successor ICON-LEPS. The impact for the minimum and maximum values for many of the parameters turned out to be important in reference to their default values and to their seasonal dependence with respect to the considered meteorological fields.

2 Work Overview

The sensitivity of ICON model was gauged over a large number (24) of parameters towards the establishment of ICON-LEPS in place of the currently operational COSMO-LEPS where model parameter perturbations are applied. The consequent list of the parameters considered of interest for the corresponding perturbations in ICON-LEPS (Table 1)has been decided and ranked according to their estimated significance by ICON experts, (Schlemmer etal, 2022) and in close reference to COSMO model (Avgoustoglou etal, 2020). All the parameters were tested over a domain covering the wider area of Greece and Italy (Figure 1 of the appendix) for a total period of four months i.e., January, April, July and October 2020 using the ICON model installed by the IsraeliMe teorological Service (IMS) at the European Center for Medium-Range Weather Forecasts (ECMWF) super-computing system and using computational resources provided gratis by the Hellenic National Meteorological Service (HNMS).
The ICON model was forced by the ECMWF operational forecast in 3-hour intervals and was performed on a 6.5 km horizontal grid for a total of approximately 6000 runs. The model sensitivities are presented for 16 surface fields over the areal average of the whole period as well as for January, April, July and October separately, at the last lead time hour (132nd) where sensitivity is expected to be on its climax.

3 Analysis

The parameters under consideration cover almost all aspects regarding the tuning of a numerical weather prediction model, i.e., turbulence, convection, terra, sub-scale orography, grid-scale micro-physics and cloud cover.

PARAMETER (meaning) relevance: high[H]/medium[M]	MIN, **DEFAULT**, MAX
P01: **a_hshr** (scale for the separated horizontal shear mode) [M]	0.1, **0.0**, 2.0
P02: **alpha0** (lower bound of velocity-dependent *Charnock* param) [H]	0.0123, **0.0123**, 0.0335
P03: **alpha1** (scaling for the molecular roughness of water waves) [H]	0.1, **0.5**, 0.9
P04: **a_stab** (stability correction of turbulent length scale factor) [M]	0.0, **0.0**, 1.0
P05: **capdcfac_et** (extratropics CAPE diurnal cycle correction) [H]	0.0, **0.5**, 1.25
P06: **c_diff** (length scale factor for vertical diffusion of TKE) [H]	0.1, **0.2**, 0.4
P07: **c_soil** (evaporating fraction of soil) [H]	0.75, **1.0**, 1.25
P08: **cwimax_ml** (scaling for maximum interception storage) [H]	0.5×10^{-7}, **1.0×10^{-6}**, 0.5×10^{-4}
P09: **entrorg** (entrainment convection scheme valid for dx=20km) [H]	0.00175, **0.00195**, 0.00215
P10: **gkwake** (low level wake drag constant for blocking) [H]	1.0 , **1.5**, 2.0
P11: **q_crit** (normalised supersaturation critical value) [H]	1.6, **2.0**, 4.0
P12: **qexc** (test parcel ascent excess grid-scale QV fraction) [M]	0.0075, **0.0125**, 0.0175
P13: **rain_n0_factor** (raindrop size distribution change) [H]	0.02 , **0.1**, 0.5
P14: **rdepths** (maximum allowed shallow convection depth) [H]	15000, **20000**, 25000
P15: **rhebc_land** (RH threshold for onset of evaporation below cloud base over land) [M]	0.70, **0.75**, 0.80
P16: **rhebc_ocean** (ibid over ocean) [H]	0.80, **0.85**, 0.90
P17: **rlam_heat_rat_sea** (scaling of laminar boundary layer for heat and latent and heat fluxes over water (constant product)) [H]	(0.25,28.0), **(1.0,7.0)**, (4.0,1.75)
P18: **rprcon** (precipitation coefficient conversion of cloud water) [H]	0.00125, **0.0014**, 0.00165
P19: **texc** (excess value for temperature used in test parcel ascent) [M]	0.075, **0.125**, 0.175
P20: **tkhmin_tkmmin** (common scaling for minimum vertical diffusion for heat-moisture and momentum) [H]	0.55 , **0.75**, 0.95
P21: **box_liq** (box width for liquid cloud diagnostic) [H]	0.03, **0.05**, 0.07
P22: **box_liq_asy** (liquid cloud diagnostic asymmetry factor) [H]	2.0 , **3.5**, 4.0
P23: **tur_len** (asymptotic maximal turbulent distance (m)) [H]	250, **300**, 350
P24: **zvz0i** (terminal fall velocity of ice) [H]	0.85 , **1.25**, 1.45

Table 1: List of the 24 parameters (P01-P24) of the tested sensitivity based on their code names, interpretation and relevance (first column) as well as their test range (second column). The default values are denoted with bold characters as well as their recommended relevance, [H] and [M] standing for high and medium respectively.

These are presented in Table 1 while in Table 2, their categorization is displayed. For every day of the considered period, forty eight 132 hour runs were performed corresponding to the minimum and maximum of the 24 examined parameters, as well as one run with the default model values (Table 1). The min/max parameter (P) sensitivity ($S_{\langle V \rangle P}$) for sixteen meteorological fields (Table 3) was evaluated according to the formula,

$$S_{\langle V \rangle P} \, (\%) = 100 \cdot \left(\frac{\langle V \rangle_P}{\langle V \rangle_D} - 1 \right) \tag{1}$$

where $\langle V \rangle$ stands for the area average of the meteorological field V over a considered period with respect to its value for the default parameter set D over the same period.

Parameter categories	Corresponding parameters
Turbulence	P01, P02, P03, P04, P06, P11, P17, P20, P23
Convection	P05, P09, P12, P14, P15, P16, P18, P19
Terra	P07, P08
Sub-Scale Orography	P10
Grid-Scale Micro-Physics	P13, P24
Cloud Cover	P21, P22

Table 2: Categorization of the parameters encoded in Table 1.

The sensitivities of the examined meteorological fields are displayed in Figures 2 to 5 of the appendix. In all figures, the parameter minimum and maximum values are placed on the horizontal axis while the corresponding sensitivities on the vertical axis. In order to have a reference regarding the actual values of the fields, the default area average value of the four month period is shown.

The sensitivities for January, April, July, October as well as the whole four month period (JAJO) are displayed respectively with blue, red, orange and black colors regarding the maximum parameter values and their corresponding lighter shades (not shown explicitly) for the minimum values. From these graphs, it is relatively straightforward to infer heuristically the parameters of the greatest sensitivity and especially the most sensitive ones for every meteorological field considered. This feature is summarized in Table 3.From this tabulation, it is important to see that these parameters are practically almost half of the 24 parameters considered overall. Even more interesting is to note that the most sensitive parameters, designated with bold characters, belong to a considerably smaller subset consisting of five parameters. Consequently, a set between five to ten parameters looks like a pragmatic and flexible choice where perturbation or optimization techniques may be applied to improve the model performance.

More specifically, regarding cloudiness (Figure 2), the most sensitive parameters for total (clct), medium (clcm) and low (clcl) cloud cover are those of P21 (box width for liquid cloud diagnostic) and P22 (liquid cloud diagnostic asymmetry factor) while for high cloud cover (clch) is clearly P24 (the terminal fall velocity of ice). Some differences with respect to seasonal sensitivity are displayed mainly for summer.

Averaged Meteorological Fields	Sensitive parameters
T2m: 2m Temperature ^{o}K	P07, P21, **P22**
Tmax2m : 2m-Temperature ^{o}K	P07, P21, **P22**, P23
T_min2m : Min 2m-Temperature ^{o}K	P17, **P20**
Td_2m : Dew point 2m-Temperature ^{o}K	**P03**, P07, P22, P23
tot_prec : Accumulated Precipitation (kg m^{-2})	P03, P17, **P22**
pmsl : Mean sea level Pressure (hPa)	P10, P21, **P22**
u10m : 10 m wind speed u component (m s^{-1})	P10, **P22**, P23
v10m : 10 m wind speed v component (m s^{-1})	P02, P10, **P22**
gust10m : Wind gust 10 m above ground (m s^{-1})	**P10**, P22, P23
clcl : Low cloud cover (1-100%)	P03, P21, **P22**
clcm : Medium cloud cover (1-100%)	P09, P14, P21, **P22**
clch : High cloud cover (1-100%)	P09, P18, P22, **P24**
clct : Total cloud cover (1-100%)	P03, P21, **P22**
tqv : Column integrated water vapor (kg m^{-2})	**P03**, P20, P22
tqi : Total column integrated cloud ice (kg m^{-2})	P18, P22, **P24**
tqc : Total column integrated cloud water (kg m^{-2})	P11, **P22**, P23

Table 3: List of the area-averaged meteorological fields over the 132nd lead time and the corresponding parameters that display great sensitivity as it can be inferred from Figures 2 to 5. The most sensitive parameter for every field is addressed with bold faced characters.

With respect to temperature (Figure 3), there are several parameters that display significant sensitivity. Nevertheless, P03 (scaling for the molecular roughness of water waves) shows the greatest sensitivity for dew-point temperature (Td2m), P20 (common scaling for minimum vertical diffusion for heat-moisture and momentum) for minimum 2m-temperature (Tmin2m) and P22 (liquid cloud diagnostic asymmetry factor) for 2m-temperature (T2m) as well as maximum 2m-temperature (Tmax2m). It can also be mentioned that there several differences in seasonal sensitivity, most of them of different magnitude but of the same sign.

The same remarks hold for the fields related to atmospheric water (Figure 4), where P22 (liquid cloud diagnostic asymmetry factor) is the most sensitive parameter regarding accumulated precipitation (tot_prec) as well as total column integrated cloud water (tqc), P03 (scaling for the molecular roughness of water waves) for total column integrated vapour (tqv) and P24 (the terminal fall velocity of ice) for total column integrated cloud ice (tqi) as expected in relevance to the same sensitivity for high cloud cover.

Referring to mean sea-level pressure (pmsl) (Figure 5, upper graph), extensive sensitivity is displayed for many parameters, however, P22 (liquid cloud diagnostic asymmetry factor) is again the most sensitive parameter. There is also extensive seasonal sensitivity for several parameters of opposite sign. The situation is practically the same for zonal (u10m) and meridional (v10m) wind components (Figure 5, bottom and upper bottom graphs). An interesting feature is related to the 10m-gust wind (gust10m) where the sensitivity is constrained essentially to P10 (low level wake drag constant for blocking) parameter.

4 Conclusions and Outlook

The impact of the minimum and maximum values for most of the parameters turned out to be important for the considered meteorological fields, in reference to their default values and to their seasonal dependence . The sensitivity was quite versatile justifying the choice to examine directly a very large number of parameters, probably one of the largest ever in a NWP model. Consequently, the advancement towards ICON-LEPS will be a formidable operational but also research challenge for the years to come that might have also some impact to ICON model overall. Due to the inclusion of a large and complicated marine area in the desired integration domain for the proposed ICON-LEPS, the project will contribute to the understanding of the behaviour of the ICON model over the Mediterranean Sea.

References

[1] Avgoustoglou, E., Voudouri, A., Carmona, I., Bucchignani, E., Levy, Y., Bettems, J. M., 2020: COSMO technical report 42. A methodology towards the hierarchy of COSMO parameter calibration tests via the domain sensitivity over the Mediterranean area: Final Report. www.cosmo-model.org, doi:DOI:10.5676/DWD_pub/nwv/cosmo-tr 42.

[2] Prill, F., Reinert, D., Rieger, D., Zängl, G., 2020: ICON Tutorial. Working with the ICON Model. https://doi.org/10.5676/dwd_pub/nwv/icon_tutorial2020

[3] Schlemmer, L., Zängl, G., Helmert, J., Köhler, M., Mironov, D., Raschendorfer, M., Reinert, D., Rieger, D., Schäfer, S., Seifert A., 2022: ICON model parameters suitable for model tuning. *Deutscher Wetterdienst (DWD), Offenbach*, http://cosmo-model.org/content/support/icon/tuning/icon-tuning.pdf

[4] of DWD and MPI-M: Description of the non-hydrostatic dynamical core. *Q. J. R. Meteorol. Soc.*, 141, **563–579**, https://doi.org/10.1002/qj.2378.

Appendix for figures 1 to 5
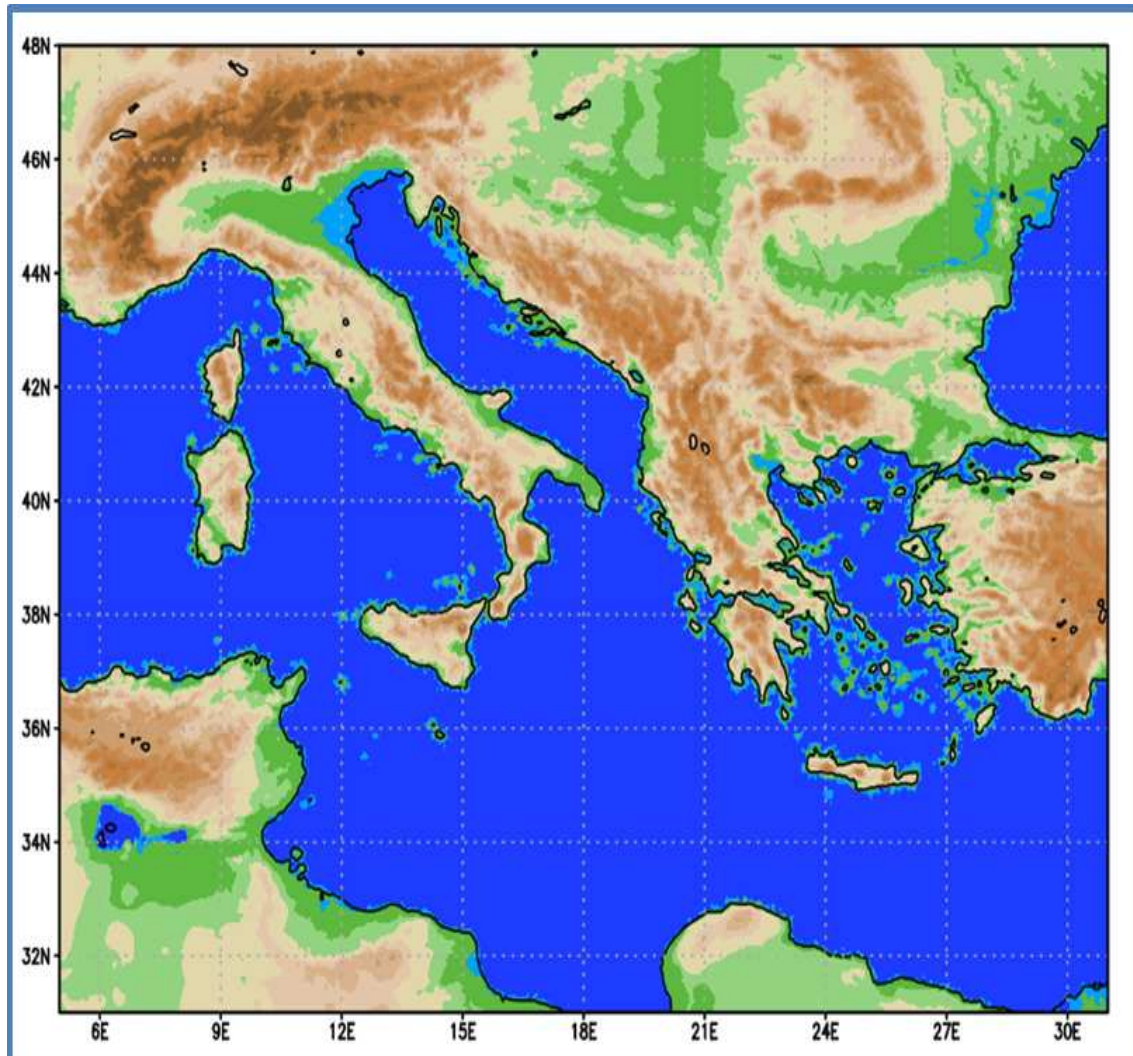
Figure 1: ICON model integration domain covering the wider area of central Mediterranean.
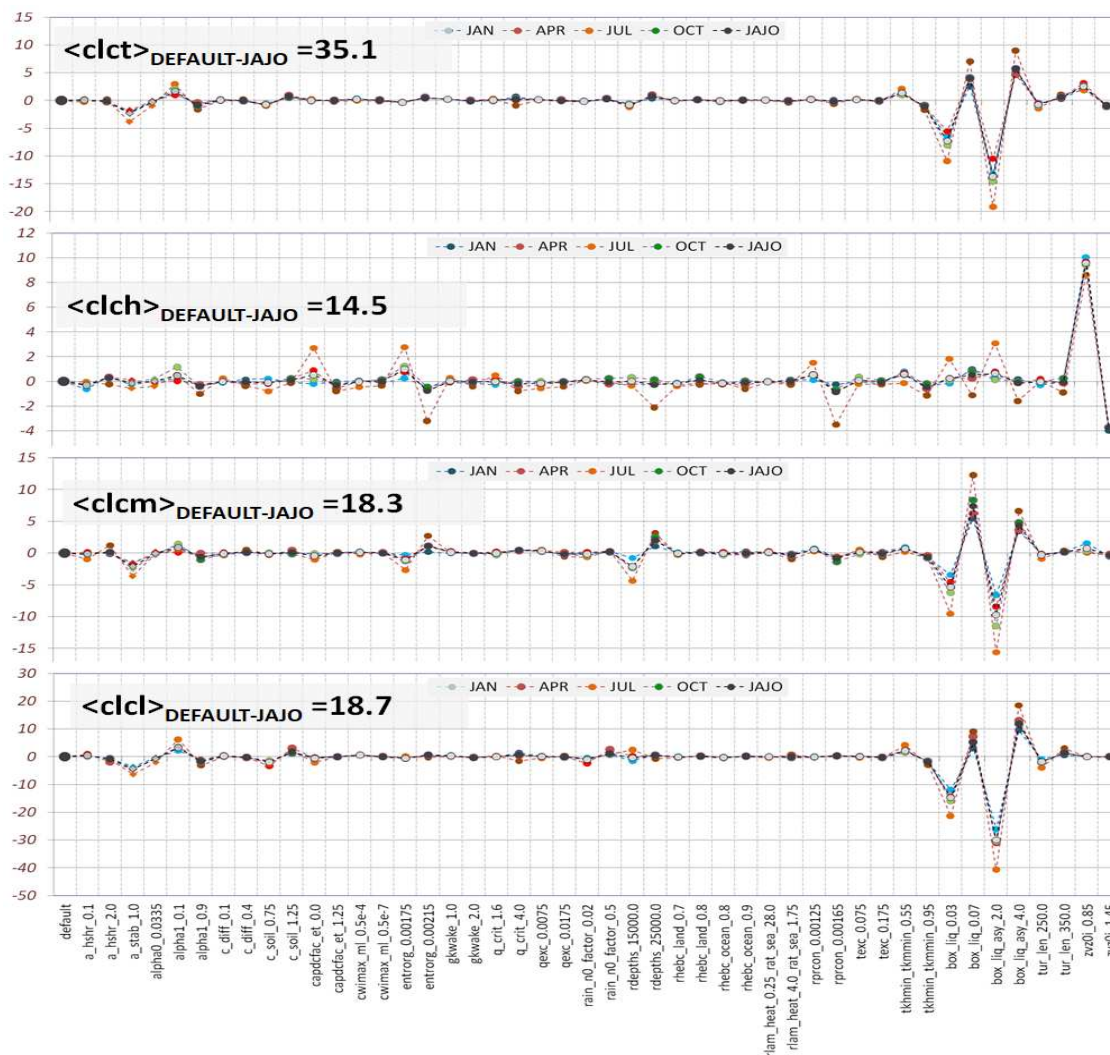
Figure 2: Area average sensitivity for total (clct), high (clch), medium (clcm) and low (clcl) cloud cover (top to bottom) for the 132nd hour of the model run. The time periods for January, April, July, October as well as thewh ole four months are displayed respectively with blue, red, orange and black colors regarding the maximum parameter values and their corresponding lighter shades (not shown explicitly) for the minimum values. The corresponding cloud cover area average values (in %) for the the default run and for the whole period are also shown (i.e, $\langle clct \rangle_{DEFAULT-JAJO}$, $\langle clch \rangle_{DEFAULT-JAJO}$, $\langle clcm \rangle_{DEFAULT-JAJO}$ and $\langle clcl \rangle_{DEFAULT-JAJO}$).
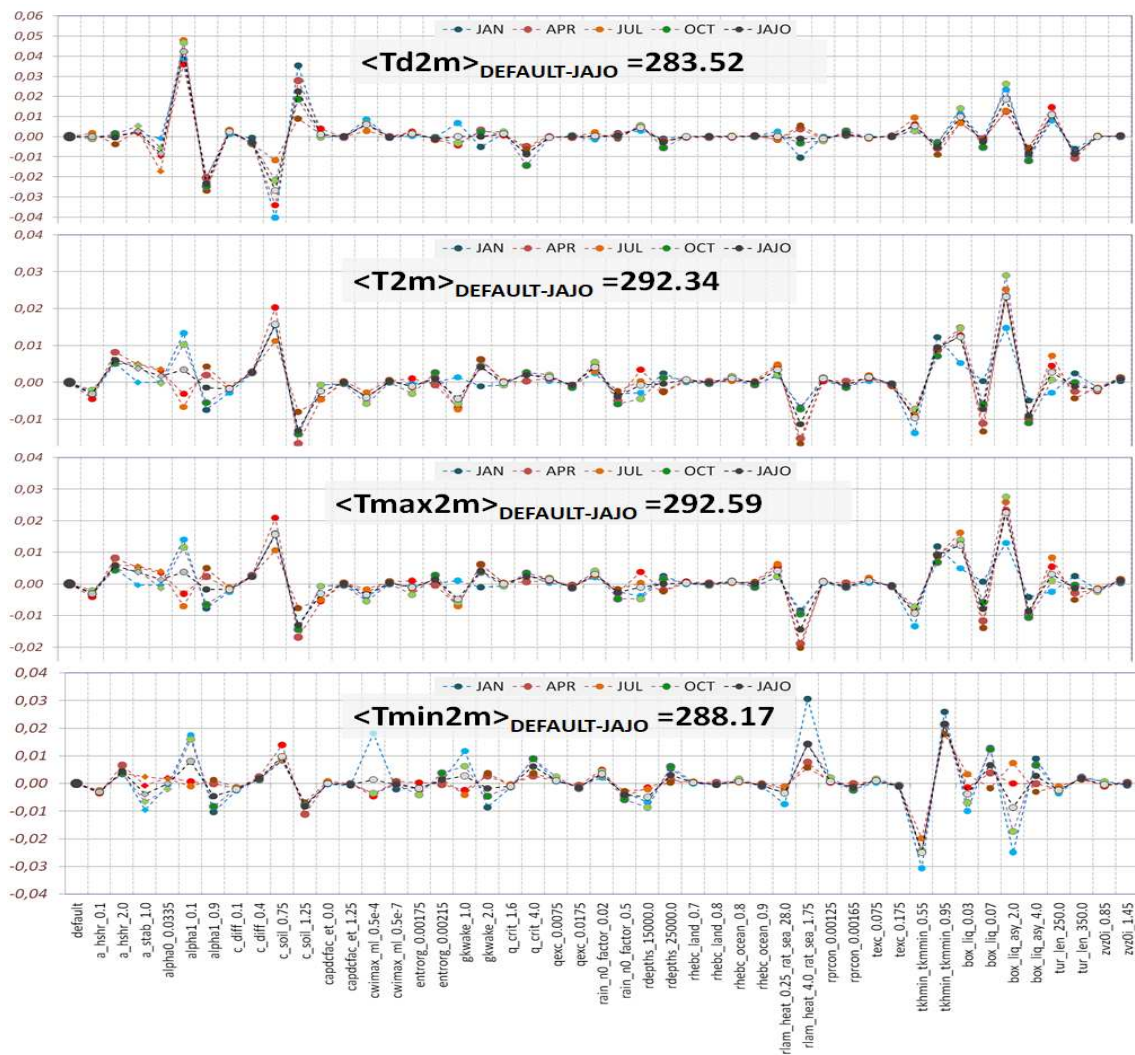
Figure 3: Area average sensitivity for dew point (Td2m), 2-meter (T2m), maximum (Tmax2m) and minimum (Tmin2m) temperature(top to bottom)for the 132nd hour of the model run. The time periods for January, April, July, October as well as the whole four months are displayed respectively with blue, red, orange and black colors regarding the maximum parameter values and their corresponding lighter shades (not shown explicitly) for the minimum values. The corresponding area average values (in ^{o}K) for the the default run and for the whole period are also shown (i.e, $\langle Td2m \rangle_{DEFAULT-JAJO}$, $\langle T2m \rangle_{DEFAULT-JAJO}$, $\langle Tmax2m \rangle_{DEFAULT-JAJO}$ and $\langle Tmin2m \rangle_{DEFAULT-JAJO}$).
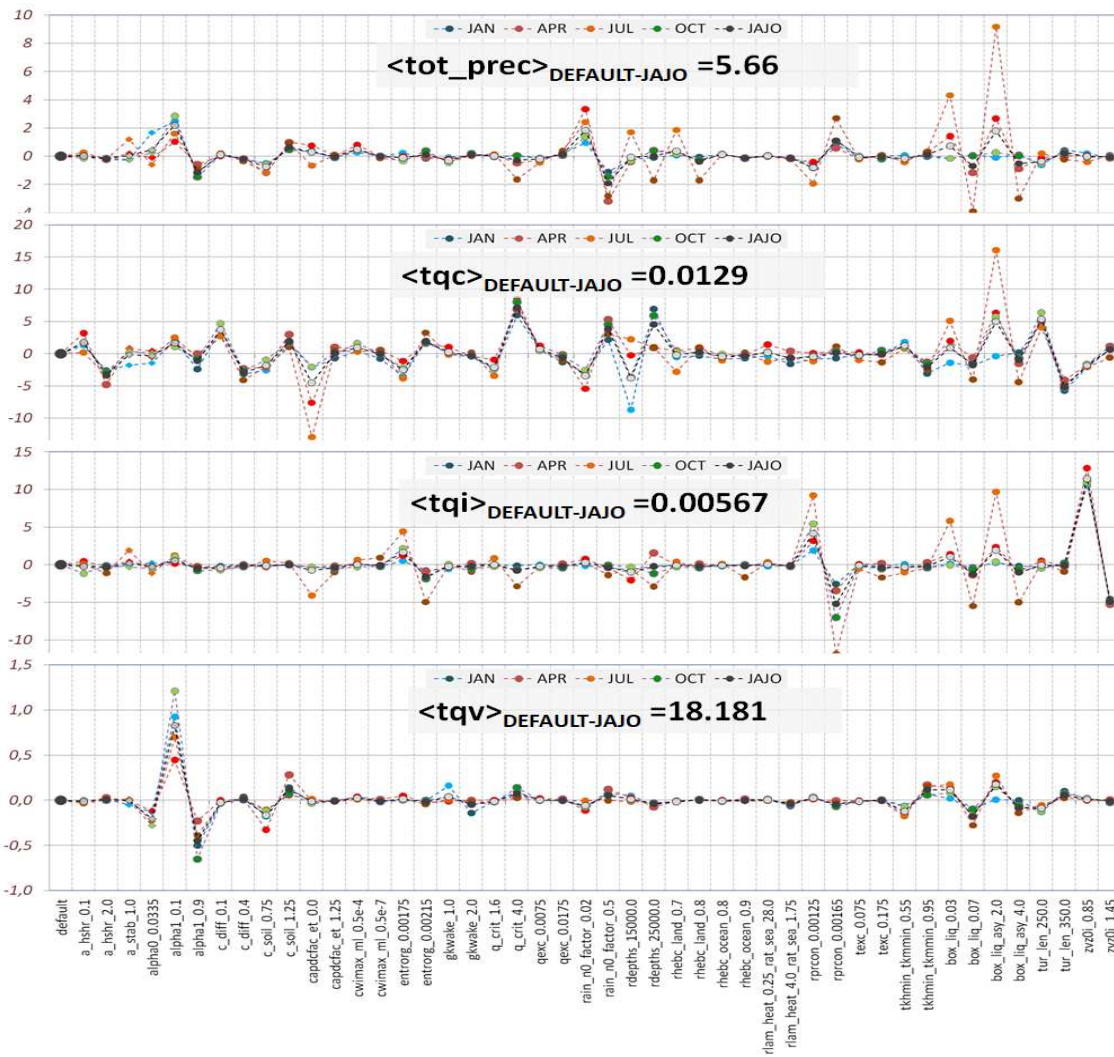
Figure 4: Area average sensitivity for accumulated precipitation (tot_prec), total column: cloud water (tqc), ice (tqi) and vapour (tqv) from top to bottom for the 132nd hour of the model run. The time periods for January, April, July, October as well as the whole four months are displayed respectively with blue, red, orange and black colors regarding the maximum parameter values and their corresponding lighter shades (not shown explicitly) for the minimum values. The corresponding area average values (in kg m^{-2}) for the the default run and for the whole period are also shown (i.e, $\langle tot_p rec \rangle_{DEFAULT-JAJO}$, $\langle tqc \rangle_{DEFAULT-JAJO}$, $\langle tqi \rangle_{DEFAULT-JAJO}$ and $\langle tqv \rangle_{DEFAULT-JAJO}$).
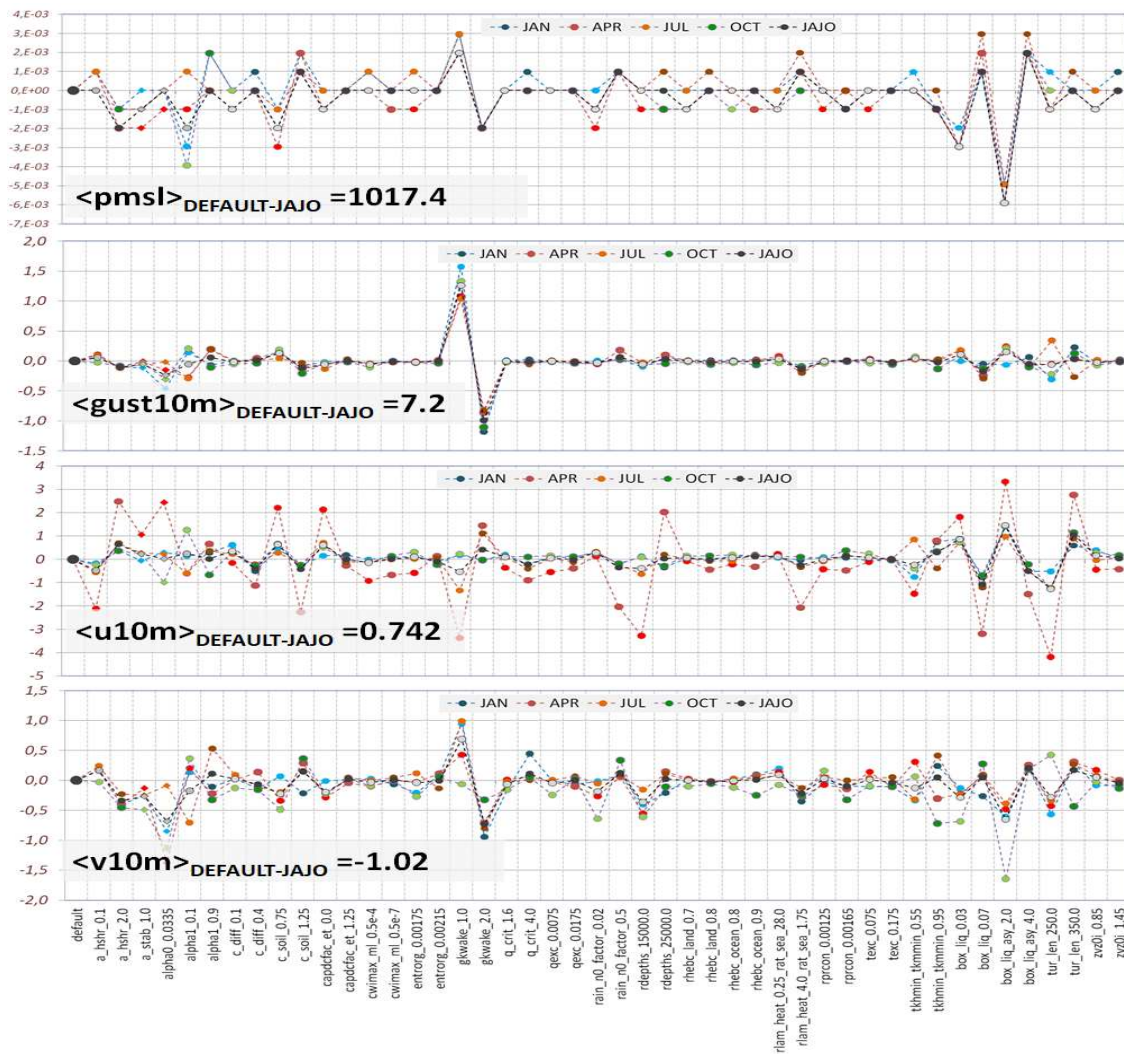
Figure 5: Area average sensitivity for mean-sea level pressure (pmsl), 10m: gust (gust10m), zonal (u10m) and meridional (v10m) wind from top to bottom for the 132nd hour of the model run. The time periods for January, April, July, October as well as the whole four months are displayed respectively with blue, red, orange and black colors regarding the maximum parameter values and their corresponding lighter shades (not shown explicitly) for the minimum values. The corresponding area average values (in hPa and m s^{-1}) for the the default run and for the whole period are also shown (i.e, $\langle pmsl \rangle_{DEFAULT-JAJO}$, $\langle gust10m \rangle_{DEFAULT-JAJO}$, $\langle u10m \rangle_{DEFAULT-JAJO}$ and $\langle v10m \rangle_{DEFAULT-JAJO}$).

Numerical Model Training Course 2023

U. Schättler[1], S. Brienen[1], F. Prill[1], D. Reinert[1], D. Rieger[1], C. Steger[1], J.-N. Welss[1] R. Dumitrache[2], S. Dinicila[2], S. Gabrian[2]

[1] *Deutscher Wetterdienst,* [2] *National Meteorological Administration, Romania*

The *Numerical Model Training Course 2023* for the ICON model took place from March 27th to 31st. The organization team from DWD received further support from the COSMO partner weather services and members of the CLM community.

The application areas of the ICON model range from numerical weather prediction (NWP) and regional climate simulations (CLM - Climate Limited Area Model) to the prediction of trace substance dispersion with ICON-ART. Therefore, national meteorological services, universities and research institutions are among the ICON users and the target groups of the training course. Each morning, lectures on the physical basics of the ICON model, data output of the DWD and technical details of ICON were scheduled (see Fig. 1). In the afternoon, practical exercises allowed participants to learn how to run ICON simulations.

Numerical Model Training 2023: Program Overview *(Times in CEST)*

	Monday 27.03.	Tuesday 28.03.	Wednesday 29.03.	Thursday 30.03.	Friday 31.03.
9:00 – 9:45		Dynamics *G. Zängl*	Microphysics *A. Seifert*	Gravity Wave Drag *M. Köhler*	Soil & External Parameters *J. Helmert*
9:45 – 10:30		Advection *D. Reinert*	Clouds & Convection *A. de Lozar*	Data Provision *H. Riede*	Lake & Sea Ice *D. Mironov*
10:30 – 11:00		Coffee Break	Coffee Break	Coffee Break	Coffee Break
11:00 – 11:45		Nesting & ICON-LAM *D. Reinert*	Turbulent Diffusion *M. Raschendorfer*	Radiation *M. Ahlgrimm*	Exercise: Installation
11:45 – 12:30		Physics Overview *L. Schlemmer*	Turbulent Transfer *M. Raschendorfer*	ICON-ART *A. Hoshyaripour*	Exercise: Installation
					Wrap-up
12:30 – 13:00	Registration	Lunch Break	Lunch Break	Lunch Break	
13:00 – 13:30	Introduction & Getting Started I *D. Rieger & F. Prill*				
13:30 – 14:00		Group Picture			
14:00 – 14:45	Getting Started II *F. Prill*	Exercise II	Exercise III	Exercise IV	
14:45 – 15:30	Exercise I	Exercise II	Exercise III	Exercise IV	
15:30 – 16:00	Coffee Break	Coffee Break	Coffee Break	Coffee Break	
16:00 – 16:45	Exercise I	Exercise II	Exercise III	Exercise IV	
16:45 – 17:30	Exercise I	Exercise II	Exercise III	Exercise IV	
17:30 –		Icebreaker			

Figure 1: Timetable for the Model Training 2023.

After the cancellation of the Numerical Model Training 2020 at short notice due to Covid 19, only a substitute online training with shortened exercises took place since then. The interest in the first face-to-face course after four years therefore was very high.

To meet this demand, three parallel exercise groups were planned already at an early stage. These groups covered NWP for universities (*Academia*), regional climate simulations (*CLM*) and NWP for national weather services (*MetServices*).

In total, we welcomed 71 participants in Offenbach (see Fig. 2). The fact that WMO supported several African national meteorological services resulted in an international course with participants from Austria, Brazil, Burkina Faso, France, Germany, Israel, Italy, Kenya, Mauritius, Mozambique, Niger, Oman, Seychelles, South Africa, Switzerland, Tanzania, United Arab Emirates and Zimbabwe.

Figure 2: Participants of Numerical Model Training 2023.

For the first time, the training was held at the headquarters in Offenbach, with exercises in the conference areas *Blue* and *Green* as well as in the *Gartensaal*. The lectures were streamed from conference area *Blue* to the other rooms.

The participants had to bring their own notebooks for the exercises. The *Academia* and CLM course were performed on the HPC `levante` at the German Climate Computing Center (DKRZ) while the *MetService* course was run on ECMWF's ATOS system.

In the scope of the training course, the ICON Tutorial was also revised and published. The ICON Tutorial is updated with each training course and is now the most comprehensive model documentation available for the ICON model.It is available for download on `https://www.dwd.de/EN/ourservices/nwv_icon_tutorial/nwv_icon_tutorial_en.html`

The exercises of the *Academia* group, designed and conducted by F. Prill, D. Reinert, and D. Rieger (DWD), cover a wide range of ICON functionalities. These exercises continue the successful ICON training that has been developed over the past ten years. A crucial innovation is the use of Jupyter Notebooks for the *Academia* exercises, which in the meantime have established themselves as the "de-facto standard" in e-learning. The initial steps consisted of idealized simulations that otherwise serve as tests with reference solution for numerical weather prediction models. By adding higher resolution simulation areas, so-called nests, the participants got to know a basic functionality of ICON, which is also used operationally, e.g. with the ICON-EU-Nest. The next step was a global three-day forecast, started from DWD analysis. Based on this, the participants extended the setup of ICON to generate initial and boundary data for a simulation with ICON as a local model (limited-area mode, LAM). In the third exercise block the LAM simulation for a higher resolution area over Germany was conducted. In the last part of the *Academia* exercises, the participants, mostly PhD students

and postdocs who want to use and further develop ICON in their projects, were able to make changes to the source code of ICON to compute and output a new diagnostic.

The CLM portion of the course was designed and delivered by the CLM community. The course provided an introduction to the *Starter Package for ICON-CLM Experiments* (SPICE). SPICE is a runtime environment for performing regional climate simulations with ICON-CLM. SPICE was developed within the CLM community. Participants learned how to install and configure SPICE and how to use it to run simulations. In special exercises the participants learned which steps are necessary to perform a simulation for a different time period, a different area and with different boundary conditions. Furthermore, it was explained how to create a simulation with convection allowing resolution. Boundary data were provided by a previously created experiment with coarser resolution. Analyzing the results with the evaluation tool *EvaSuite* included in SPICE has been explained as well. In the final exercise, participants were able to begin configuring the model for their target region and use case.

For the first time, tailored exercises with the ICON model were offered for the group of national meteorological services. These exercises and corresponding materials have been developed by a group of COSMO scientists: U. Schättler and J.-N. Welß from DWD, S. Dinicila, S. Gabrian and R. Dumitrache from NMA, W. Interewicz and D. Wojcek from IMGW and A. Shtivelman from IMS. Several online meetings have been held in the weeks before the NWP Model Training to coordinate and discuss the necessary work. The first task for the participants was to generate a grid and external parameters for their own model area using the DWD's grid generator web service. The preprocessing step (interpolation of global ICON data to a regional grid) and the execution of an ICON-LAM simulation were then performed by all of them on a provided grid under the guidance of the tutors. Subsequently, these steps then had to be transferred to the self-generated grid in the individual participants target area. Exercises for visualizing the model results rounded off the practical learning content. On the last afternoon, colleagues from ECMWF offered online lectures and exercises on ECMWF's scheduler `ecflow`. This enables the automated execution of all steps that were started by hand during this week, which is necessary for an operational prediction. All computer simulations were performed on DWD training accounts on ECMWF's HPC (ATOS).

The final exercise block, common to all groups, provided an overview of how to install ICON on an HPC system. This exercise was designed and performed by U. Schättler.

We would like to express our sincere thanks to all colleagues who supported us in the preparation and execution. Special thanks go to ECMWF for their support with ecflow and the HPC system.

ICCARUS 2023

Daniel Rieger and Christian Steger

ICCARUS 2023

ICCARUS (ICON/COSMO/CLM/ART User Seminar) is an international conference that brings together users and developers of the COSMO and ICON numerical models. Over the last two decades ICCARUS has become a hub for the exchange of information on model development, physical parameterizations, data assimilation, ensemble generation, verification and applications of the model systems. As such, it provides an important link between COSMO, the CLM community, and ICON and ART developers.

The 24th edition of ICCARUS took place from 6 - 9 March 2023 at the DWD headquarters in Offenbach, Germany. The conference was planned and executed for the first time as a hybrid event by the organization team consisting of Anja Thomas, Daniel Egerer, Bernd Kress, Daniel Rieger, and Christian Steger. For this, the proven tools Webex, Gather.Town and Nextcloud could be used.

After greetings by DWD President Prof. Gerhard Adrian and the head of DWD's research and development business unit, Prof. Sarah Jones, the first three days of the conference featured scientific presentations in plenary sessions. These could be followed and given on-site as well as online. The poster session then took place entirely online on Thursday 9 March. There was the possibility to present the posters in short presentations in the plenum on Monday and Tuesday. The working group meetings of COSMO, the CLM and the ICON community, which used to be held during the ICCARUS week in Offenbach as well, were now held as virtual meetings in the weeks before and after. The only element of the conference which was exclusively reserved for on-site participants was the Icebreaker event, which took place following the scientific program on Tuesday evening.

A total of 286 people were registered for ICCARUS 2023, of which 110 were registered for on-site participation. Participants submitted 88 papers, of which 42 were oral presentations and 46 were poster presentations. The plenary presentations were organized into a total of 14 thematic sections. These included "Aerosol and Clouds", "Coupled Simulations", "Predictabilty", "Boundary Layer and Soil", "Data Assimilation", "Clouds and Convection", "SINFONY", "Model Development", "Radiation", "Dynamic and Numerical", "Aerosol", "Evaluation", "Dynamic and Gravity Waves" and "Clouds". For the division of the thematic blocks, the keyword system introduced in the previous year again proved helpful for the submission of contributions.

The program also included 5 keynote talks, including an invited talk by Stephanie Johnson (ECMWF) on ECMWF's seasonal forecasting system. The other four keynote talks were given by colleagues of DWD and dealt with various aspects of the ICON model system. Roland Potthast gave a general overview of ongoing work and plans with ICON. Jan Keller presented the regional re-analysis generated by DWD in more detail. Günther Zängl explained the major updates in ICON for weather forecasting, as well as the related plans for 2023. Barbara Früh provided information on the work for using ICON on climate time scales.

The programme, the book of abstracts, and many presentations and posters can be found on the `https://www.dwd.de/EN/specialusers/research_education/seminar/2023/iccarus2023/iccarus_2023_en_node.html`

Next year ICCARUS will celebrate its 25th anniversary and will be held during the week of March 4-9, 2024.

Figure 1: ICCARUS 2023 Logo (Source: Nora Leps)

Figure 2: Group picture

Dear COSMO colleagues,

After nearly three years of virtual meetings, we met again in the cradle of modern civilization, Athens. We all enjoyed a very fruitful and joyful General Meeting (thanks, HNMS) and found out that the COSMO spirit was not lost, and a great deal of good work was accomplished.

It is now one year after the last COSMO Version 6.0 has been completed and the PP C2I successfully led by Daniel Rieger (DWD) brought our services to run and use ICON-LAM. We still need to complete the migration of our EPSs (PP PROPHECY) and port the ICON code to GPU (PP IMPACT). The COSMO-LEPS, which was initiated 20 years ago, is getting renewed by Ines Cerenzia (ARPAE). ICON-LEPS will run on the new ATOS machine in Bologna and there are plans to upgrade LEPS to convection-permitting resolution in a domain including all of the Mediterranean Sea. With PPCARMENs we hopefully will be able to evaluate all our EPSs and visualise the results as a tool for improving future EPS results.

One of the main challenges of COSMO is to migrate COSMO users around the world to ICON-LAM and to develop a global ICON-LAM user community. Many contributors to PPC2I4LC led by Bogdan Maco (NMA), PPCOMFORT led by Dimitra Boucouvala (HNMS) and PPWG6-SPRT led by Massimo Milelli (CIMA) are working to achieve this goal.

The main goal of regional models is to downscale coarse global models. As computer power develops and global models are increasing resolution we need to invest all our scientific efforts to produce sub-Km resolution ICON-LAM. Such a task requires combined forces of COSMO scientists (PP's KENDAScope, CITTA, CAIIR, MILEPOST, and include other projects like BRIDGE, TEAMx and GLORI.

I would like to take this opportunity to thank key positions in COSMO:

- Working group coordinators and PP leaders in charge of COSMO's scientific and organizational work.
- Christoph Gebhardt (DWD), for his enthusiasm, devotion and wonderful work as COSMO SPM.
- Panagiotis Skrimizeas (HNMS), who volunteered to serve as COSMO chair of STC for the next two years.

Their success is COSMO's success.

2022 will be remembered by the outburst of the brutal war in Ukraine. As with any other war, all parties seem to be losing much more than they can possibly gain. It seems that this war is yet another example of human irrational decisions. Let's pray and hope that in 2023 the decision-makers will not try to invest more human lives to compensate for those already sacrificed and struggle for a fast, peaceful solution to this human-made crisis so COSMO can work again with all its scientific power.

Yoav Levi IMS
Chair of COSMO steering committee (STC) 2021-2022.

The contribution of COSMO members IMS and CIMA to humanitarian cooperation in Ukraine

Davide Miozzo, Sabrina Meninno, Giorgio Meschi, Fabio Violante, Rocco Masi, Martina Lagasio, Massimo Milelli (all CIMA Research Foundation), Lorenzo Massucchielli (Italian Red Cross), Yoav Levi, Pavel Khain, Alon Shtivelman, Nir Stav (all Israel Meteorological Service), Sari Lappi (WMO), Umberto Modigliani (ECMWF)

In the framework of the EU-funded programme for Prevention, Preparedness and Response to natural and man-made disasters in Eastern Partnership countries - phase 3 (PPRD East 3), ECMWF, CIMA and IMS collaborated to release a daily Impact-Based Forecast Bulletin (IBF) over Ukraine. The IBF combines information on weather variables, encompassing low temperatures, rain, wind, snow, and biometric indices, with data on particular vulnerabilities. In particular, weather data are retrieved from the numerical weather prediction model ICON run by the Israel Meteorological Service (IMS) and the IBF has been built up with the help of CIMA expertise and the local Met Service.

The ICON model provides data with a horizontal resolution of 2.5 kilometres and a temporal resolution of 1 hour. Data are then aggregated in time and space over Ukrainian Oblasts and classified in colour-coded categories. They thus show alert levels to convey hazard information that is immediately identifiable, recognisable and comprehensible by non-experts working on the ground (e.g., International Red Cross).

For more information on the IBF, see https://www.ecmwf.int/sites/default/files/elibrary/012023/81350-newsletter-no-175-spring-2023.pdf

For more info about the project PPRD East 3, see https://www.pprdeast3.eu/

List of COSMO Newsletters and Technical Reports

(available for download from the COSMO Website: `www.cosmo-model.org`)

COSMO Newsletters

No. 1: February 2001.

No. 2: February 2002.

No. 3: February 2003.

No. 4: February 2004.

No. 5: April 2005.

No. 6: July 2006; Proceedings from the COSMO General Meeting 2005.

No. 7: May 2008; Proceedings from the COSMO General Meeting 2006.

No. 8: August 2008; Proceedings from the COSMO General Meeting 2007.

No. 9: December 2008; Proceedings from the COSMO General Meeting 2008.

No.10: January 2010; Proceedings from the COSMO General Meeting 2009.

No.11: February 2011; Proceedings from the COSMO General Meeting 2010.

No.12: March 2012; Proceedings from the COSMO General Meeting 2011.

No.13: April 2013; Proceedings from the COSMO General Meeting 2012.

No.14: April 2014; Proceedings from the COSMO General Meeting 2013.

No.15: July 2015; Proceedings from the COSMO General Meeting 2014.

No.16: June 2016; Proceedings from the COSMO General Meeting 2015.

No.17: July 2017; Proceedings from the COSMO General Meeting 2016.

No.18: November 2018; Proceedings from the COSMO General Meeting 2017.

No.19: October 2019; Proceedings from the COSMO General Meeting 2018.

No.20: November 2020; Proceedings from the COSMO General Meeting 2019.

No.21: May 2022; Proceedings from the COSMO General Meeting 2021.

No.22: May 2023; Proceedings from the COSMO General Meeting 2022.

COSMO Technical Reports

No. 1: Dmitrii Mironov and Matthias Raschendorfer (2001):
        Evaluation of Empirical Parameters of the New LM Surface-Layer Parameterization Scheme. Results
        from Numerical Experiments Including the Soil Moisture Analysis.

No. 2: Reinhold Schrodin and Erdmann Heise (2001):
        The Multi-Layer Version of the DWD Soil Model TERRA_LM.

No. 3: Günther Doms (2001):
        A Scheme for Monotonic Numerical Diffusion in the LM.

No. 4: Hans-Joachim Herzog, Ursula Schubert, Gerd Vogel, Adelheid Fiedler and Roswitha Kirchner (2002):
        LLM ⁻ the High-Resolving Nonhydrostatic Simulation Model in the DWD-Project LITFASS.
        Part I: Modelling Technique and Simulation Method.

No. 5: Jean-Marie Bettems (2002):
        EUCOS Impact Study Using the Limited-Area Non-Hydrostatic NWP Model in Operational Use at
        MeteoSwiss.

No. 6: Heinz-Werner Bitzer and Jürgen Steppeler (2004):
        Description of the Z-Coordinate Dynamical Core of LM.

No. 7: Hans-Joachim Herzog, Almut Gassmann (2005):
        Lorenz- and Charney-Phillips vertical grid experimentation using a compressible nonhydrostatic toy-model relevant to the fast-mode part of the 'Lokal-Modell'

No. 8: Chiara Marsigli, Andrea Montani, Tiziana Paccagnella, Davide Sacchetti, André Walser, Marco Arpagaus, Thomas Schumann (2005):
        Evaluation of the Performance of the COSMO-LEPS System

No. 9: Erdmann Heise, Bodo Ritter, Reinhold Schrodin (2006):
        Operational Implementation of the Multilayer Soil Model

No. 10: M.D. Tsyrulnikov (2007):
        Is the particle filtering approach appropriate for meso-scale data assimilation?

No. 11: Dmitrii V. Mironov (2008):
        Parameterization of Lakes in Numerical Weather Prediction. Description of a Lake Model.

No. 12: Adriano Raspanti (2009):
        Final report on priority project VERSUS (VERification System Unified Survey).

No. 13: Chiara Mirsigli (2009):
        Final report on priority project SREPS (Short Range Ensemble Prediction System).

No. 14: Michael Baldauf (2009):
        COSMO Priority Project "Further Developments of the Runge-Kutta Time Integration Scheme" (RK); Final Report.

No. 15: Silke Dierer (2009):
        COSMO Priority Project "Further Developments of the Runge-Kutta Time Integration Scheme" (RK); Final Report.

No. 16: Pierre Eckert (2009):
        COSMO Priority Project "INTERP"; Final Report.

No. 17: D. Leuenberger, M. Stoll, A. Roches (2010):
        Description of some convective indices, implemented in the COSMO model.

No. 18: Daniel Leuenberger (2010):
        Statistical Analysis of high-resolution COSMO Ensemble forecasts, in view of Data Assimilation.

No. 19: A. Montani, D. Cesari, C. Marsigli, T. Paccagnella (2010):
        Seven years of activity in the field of mesoscale ensemble forecasting by the COSMO-LEPS system: main achievements and open challenges.

No. 20: A. Roches, O. Fuhrer (2012):
        Tracer module in the COSMO model.

No. 21: M. Baldauf (2013):
        A new fast-waves solver for the Runge-Kutta dynamical core.

No. 22: C. Marsigli, T. Diomede, A. Montani, T. Paccagnella, P. Louka, F. Gofa, A. Corigliano (2013):
        The CONSENS Priority Project.

No. 23: M. Baldauf, O. Fuhrer, M. J. Kurowski, G. de Morsier, M. Muellner, Z. P. Piotrowski, B. Rosa, P. L. Vitagliano, D. Wojcik, M. Ziemianski (2013):
        The COSMO Priority Project 'Conservative Dynamical Core' Final Report.

No. 24: A. K. Miltenberger, A. Roches, S. Pfahl, H. Wernli (2014):
        Online Trajectory Module in COSMO: A short user guide.

No. 25: P. Khain, I. Carmona, A. Voudouri, E. Avgoustoglou, J.-M. Bettems, F. Grazzini (2015):
        The Proof of the Parameters Calibration Method: CALMO Progress Report.

No. 26: D. Mironov, E. Machulskaya, B. Szintai, M. Raschendorfer, V. Perov, M. Chumakov, E. Avgoustoglou (2015):
The COSMO Priority Project 'UTCS' Final Report.

No. 27: Jean-Marie Bettems (2015):
The COSMO Priority Project 'COLOBOC' Final Report.

No. 28: Ulrich Blahak (2016):
RADAR_MIE_LM and RADAR_MIELIB - Calculation of Radar Reflectivity from Model Output.

No. 29: M. Tsyrulnikov, D. Gayfulin (2016):
A Stochastic Pattern Generator for ensemble applications.

No. 30: Dmitrii Mironov, Ekaterina Machulskaya (2017):
A Turbulence Kinetic Energy - Scalar Variance Turbulence Parameterization Scheme.

No. 31: P. Khain, I. Carmona, A. Voudouri, E. Avgoustoglou, J.-M. Bettems, F. Grazzini, P. Kaufmann (2017):
CALMO - Progress Report.

No. 32: A. Voudouri, P. Khain, I. Carmona, E. Avgoustoglou, J.M. Bettems, F. Grazzini, O. Bellprat, P. Kaufmann and E. Bucchignani (2017):
Calibration of COSMO Model, Priority Project CALMO Final report.

No. 33: Naim Vela (2017):
V.A.S.T. (Versus Additional Statistical Techniques) User Manual (v2.0).

No. 34: C. Marsigli, D. Alferov, M. Arpagaus, E. Astakhova, R. Bonanno, G. Duniec, C. Gebhardt, W. Interewicz, N. Loglisci, A. Mazur, V. Maurer, A. Montani, A. Walser (2018):
COsmo Towards Ensembles at the Km-scale IN Our countries" (COTEKINO), Priority Project final report.

No. 35: G. Rivin, I. Rozinkina, E. Astakhova, A. Montani, D. Alferov, M. Arpagaus, D. Blinov, A. Bundel, M. Chumakov, P. Eckert, A. Euripides, J. Foerstner, J. Helmert, E. Kazakova, A. Kirsanov, V. Kopeikin, E. Kukanova, D. Majewski, C. Marsigli, G. de Morsier, A. Muravev, T. Paccagnella, U. Schaettler, C. Schraff, M. Shatunova, A. Shcherbakov, P. Steiner, M. Zaichenko (2017):
The COSMO Priority Project CORSO Final Report.

No. 36: A. Raspanti, A. Celozzi, A. Troisi, A. Vocino, R. Bove, F. Batignani(2018):
The COSMO Priority Project VERSUS2 Final Report

No. 37: INSPECT Final Report A. Bundel, F. Gofa, D. Alferov, E. Astakhova, P. Baumann, D. Boucouvala, U. Damrath, P. Eckert, A. Kirsanov, X. Lapillonne, J. Linkowska, C. Marsigli, A. Montani, A. Muraviev, E. Oberto, M.S. Tesini, N. Vela, A. Wyszogrodzki, M. Zaichenko, A. Walser(2019):
The COSMO Priority Project INSPECT Final Report

No. 38: G. Rivin, I. Rozinkina, E. Astakhova, A. Montani, J-M. Bettems, D. Alferov, D. Blinov, P. Eckert, A. Euripides, J. Helmert, M.Shatunova(2019):
The COSMO Priority Project CORSO-A Final Report

No. 39: C. Marsigli, D. Alferov, E. Astakhova, G. Duniec, D. Gayfulin, C. Gebhardt, W. Interewicz, N. Loglisci, F. Marcucci, A. Mazur, A. Montani, M. Tsyrulnikov, A. Walser (2019):
Studying perturbations for the representation of modeling uncertainties in Ensemble development (SPRED Priority Project): Final Report

No. 40: E. Bucchignani, P. Mercogliano, V. Garbero, M. Milelli, M. Varentsov, I. Rozinkina, G. Rivin, D. Blinov, A. Kirsanov, H. Wouters, J.-P. Schulz, U. Schaettler (2019)
Analysis and Evaluation of TERRA_URB Scheme: PT AEVUS Final Report

No. 41: X. Lapillonne, O. Fuhrer (2020)
Performance On Massively Parallel Architectures (POMPA): Final report

No. 42: E. Avgoustoglou, A. Voudouri, I Carmona, E. Bucchignani, Y. Levy, J. -M. Bettems (2020)
A methodology towards the hierarchy of COSMO parameter calibration tests via the domain sensitivity over the Mediterranean area

No. 43: H. Muskatel, U. Blahak, P. Khain, A. Shtivelman, M. Raschendorfer, M. Kohler, D. Rieger, O. Fuhrer, X. Lapillonne, G. Rivin, N. Chubarova, M. Shatunova, A. Poliukhov, A. Kirsanov, T. Andreadis, S. Gruber (2021)
The COSMO Priority Project T2(RC)2: Testing and Tuning of Revised Cloud Radiation Coupling, Final Report

No. 44: M. Baldauf, D. Wojcik, F. Prill, D. Reinert, R. Dumitrache, A. Iriza, G. deMorsier, M. Shatunova, G. Zaengl, U. Schaettler (2021)
The COSMO Priority Project CDIC: Comparison of the dynamical cores of ICON and COSMO, Final Report

No. 45: Marsigli C., Astakhova E., Duniec G., Fuezer L., Gayfulin D., Gebhardt C., Golino R., Heppelmann T., Interewicz W., Marcucci F., Mazur A., Sprengel M., Tsyrulnikov M., Walser A.
The COSMO Priority Project APSU: Final Report

No. 46: A. Iriza-Burca, F. Gofa, D. Boucouvala, T. Andreadis, J. Linkowska, P. Khain, A. Shtivelman, F. Batignani, A. Pauling, A. Kirsanov, T. Gastaldo, B. Maco, M. Bogdan, F. Fundel
The COSMO Priority Project CARMA: Common Area with Rfdbk/MEC Application Final Report

No. 47: A. Voudouri, E. Avgoustoglou, Y. Levy, I. Carmona, E. Bucchignani, J.-M. Bettems
Calibration of COSMO Model, Priority Project CALMO-MAX: Final Report

No. 48: D. Rieger et al.
The Priority Project C2I, Transition of COSMO to ICON - Final Report

No. 49: E. Churiulin, M. Toelle, V. Kopeikin, M. Uebel, J. Helmert and J.-M. Bettems
The COSMO Priority Task VAINT:Vegetation Atmosphere INTeractions Report